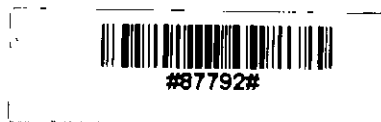


STUDY OF THE EFFECT OF NON-UNIFORM FM RESPONSE OF DFB-LD ON OPTICAL CPFSK HETERODYNE DELAY-DEMODULATION SYSTEM

A Thesis submitted to the Electrical and Electronic
Engineering Department of BUET, Dhaka,
in partial fulfilment of the
requirements for the degree of
Master of Science in Engineering
(Electrical and Electronic)



M. NAZRUL ISLAM



August 1994

R.
623.8412
1994
NAZ

DECLARATION

I hereby declare that this work has not been submitted elsewhere for the award of any degree or diploma or for publication.

M. Nazrul Islam.

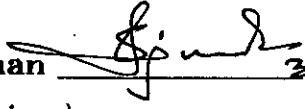
(M. Nazrul Islam)

APPROVAL


The thesis titled "STUDY OF THE EFFECT OF NON-UNIFORM FM RESPONSE OF DFB-LD ON OPTICAL CPFSK HETERODYNE DELAY-DEMODULATION SYSTEM" submitted by M. Nazrul Islam, Roll No. 901321P, session 1988-'89 to the Electrical and Electronic Engineering Department of B.U.E.T. has been accepted as satisfactory for partial fulfilment of the requirements for the degree of Master of Science in Engineering (Electrical and Electronic).

Board of Examiners

1. Dr. S. P. Majumder
Assistant Professor
Department of EEE
B.U.E.T., Dhaka 1000

Chairman  31-8-94
(Supervisor)

2. Dr. Syed Fazl-i Rahman
Professor and Head
Department of EEE
B.U.E.T., Dhaka 1000

Member  31-8-94
(Ex-officio)

3. Dr. Kazi Mohiuddin Ahmed
Associate Professor
Department of EEE
B.U.E.T., Dhaka 1000

Member  31/8/94

4. Dr. Shamsuddin Ahmed
Head
Department of EEE
ICTVTR, Gazipur, Dhaka

Member  31/08/94
(External)

ACKNOWLEDGEMENT

The author expresses his sincere and profound gratitude to Dr. Satya Prasad Majumder, Assistant Professor of Electrical and Electronic Engineering Department of BUET for his incessant and meticulous guidance in completing this work. The author thanks him for his outstanding suggestions and help during vital phases of the work.

The author wishes to express his thanks and regards to Dr. Syed Fazl-i Rahman, Professor and Head of the Electrical and Electronic Engineering Department, BUET for his encouragement and cooperation to complete this work successfully.

The author also wishes to express his thanks to Dr. Mohammad Ali Choudhury for his helpful suggestions. Sincerest thanks to Faizul Alam, Md. Mohsin Mollah and all other friends and colleagues for their cooperation and encouragement.

CONTENTS

| | |
|-------------------------------------|-------|
| DECLARATION | (i) |
| APPROVAL | (ii) |
| ACKNOWLEDGEMENT | (iii) |
| CONTENTS | (iv) |
| LIST OF PRONCIPAL SYMBOLS | (vii) |
| LIST OF ABBREVIATIONS | (ix) |
| LIST OF FIGURES | (xi) |
| ABSTRACT | (xiv) |

Chapter 1: INTRODUCTION

| | | |
|-----|--|----|
| 1.1 | Communication System | 1 |
| 1.2 | Optical Communication | 3 |
| | 1.2.1 Optical Sources | 6 |
| | 1.2.2 Optical Detectors | 7 |
| | 1.2.3 Detection Schemes | 8 |
| | 1.2.4 Modulation Schemes | 8 |
| 1.3 | Brief Review of Previous Works | 10 |
| 1.4 | Objective of the thesis | 12 |
| 1.5 | Organization of the thesis | 12 |

Chapter 2: OPTICAL HETERODYNE CPFSK RECEIVER WITH DELAY-DEMODULATION

| | | |
|-----|--|----|
| 2.1 | Introduction | 14 |
| 2.2 | Performance Limitations | 15 |
| | 2.2.1 Non-uniform FM Response of DFB Laser | 15 |
| | 2.2.2 Laser Phase Noise | 19 |

| | | |
|-------|--|----|
| 2.2.3 | Local Oscillator Excess Noise | 21 |
| 2.2.4 | Receiver Noise | 21 |
| 2.2.5 | Polarization Problems | 22 |
| 2.3 | Receiver Model | 22 |
| 2.4 | Theoretical Analysis | 24 |
| 2.4.1 | The Optical Signal | 24 |
| 2.4.2 | Noise Processes $n(t)$ and $\phi_n(t)$ | 26 |
| 2.4.3 | Output Phase of IF Filter | 27 |
| 2.4.4 | Delay-demodulation with Uniform LD FM Response | 29 |
| 2.4.5 | Delay-demodulation with Non-uniform LD FM Response | 30 |
| 2.4.6 | Data Decision | 32 |
| 2.4.7 | Bit Error Rate | 33 |
| 2.5 | Optical CPFSK with Linecoding | 35 |
| 2.5.1 | AMI Linecoding | 35 |
| 2.5.2 | BER with AMI Linecoding | 35 |
| 2.6 | Results and Discussions | 37 |
| 2.7 | Summary | 55 |

**Chapter 3: SIMULATION OF OPTICAL CPFSK HETERODYNE
RECEIVER WITH DELAY-DEMODULATION**

| | | |
|-------|--|----|
| 3.1 | Introduction | 56 |
| 3.2 | Modified Monte-Carlo Simulation | 57 |
| 3.2.1 | Biasing a Gaussian Pdf | 57 |
| 3.2.2 | Weighting Factor | 59 |
| 3.3 | Steps of Simulation | 60 |
| 3.3.1 | Generation of IF Signal Samples | 60 |
| 3.3.2 | Generation of Bit Sequence | 61 |
| 3.3.3 | Generation of Angle Modulation Samples | 61 |

| | | |
|-------|---|----|
| 3.3.4 | Generation of Phase Noise Samples | 63 |
| 3.3.5 | Generation of Noise Samples | 63 |
| 3.3.6 | IF Filtering | 64 |
| 3.3.7 | Delay-demodulation | 64 |
| 3.3.8 | Computation of BER | 65 |
| 3.4 | Results and Discussions | 65 |
| 3.5 | Summary | 71 |

Chapter 4: CONCLUSIONS AND SUGGESTIONS

| | | |
|-----|-----------------------|----|
| 4.1 | Conclusions | 72 |
| 4.2 | Suggestions | 74 |

| | |
|-----------------------------|-----------|
| REFERENCES | 75 |
|-----------------------------|-----------|

| | |
|---------------------------|------------|
| APPENDIX | A-1 |
|---------------------------|------------|

LIST OF PRINCIPAL SYMBOLS

| | | |
|----------------|---|-----------------------------------|
| $m(t)$ | = | Impulse response of laser |
| $M(f)$ | = | FM response of laser |
| Δf | = | Peak frequency deviation |
| $\delta(t)$ | = | Delta dirac function |
| T | = | Bit period |
| R_b | = | Bit rate |
| B_{IF} | = | IF bandwidth |
| $s(t)$ | = | Optical signal |
| P_s | = | Optical signal power |
| ω_c | = | Carrier frequency |
| $\phi_s(t)$ | = | Angle modulation |
| $\phi_{nT}(t)$ | = | Phase noise of transmitting laser |
| $\phi_{LO}(t)$ | = | Phase noise of local oscillator |
| $\phi_n(t)$ | = | Composite phase noise |
| $I(t)$ | = | NRZ information bit sequence |
| a_n | = | n th information bit |
| $p(t)$ | = | Elementary pulse shape |
| ω_{IF} | = | IF centre frequency |
| R | = | Responsivity of photodetector |
| $n(t)$ | = | Additive white Gaussian noise |

| | | |
|--------------|---|---|
| N_o | = | Noise spectral density |
| ρ | = | IF signal-to-noise ratio |
| S | = | IF signal amplitude |
| B | = | Baseband bandwidth of transmitted signal |
| $h(t)$ | = | Impulse response of normalized equivalent filter |
| h | = | FSK modulation index |
| τ | = | Time delay for delay-demodulation |
| $\theta(t)$ | = | Phase error of demodulated signal from desired phase |
| $P_e \theta$ | = | Error probability conditioned on $\theta(t)$ |
| P_e | = | Unconditional bit error probability |
| $f_X(x)$ | = | Pdf of noise process |
| $g_X(x)$ | = | Pdf of biased noise process |
| $B(X_k)$ | = | Biassing factor of noise X_k |
| N_{SB} | = | No. of samples per bit |
| σ^2 | = | Variance |
| β | = | Linewidths |

LIST OF ABBREVIATIONS

| | | |
|--------|---|------------------------------|
| ASK | = | Amplitude shift keying |
| APD | = | Avalanche photodetector |
| AMI | = | Alternate-Mark-Inversion |
| BER | = | Bit error rate |
| BW | = | Bandwidth |
| CNR | = | Carrier-to-noise ratio |
| CPFSK | = | Continuous phase FSK |
| DFB | = | Distributed feedback |
| DFB-LD | = | Distributed feedback LD |
| DFT | = | Discrete Fourier transform |
| DPFSK | = | Discontinuous phase FSK |
| DPSK | = | Differential PSK |
| EMI | = | Electromagnetic interference |
| FFT | = | Fast Fourier transform |
| FM | = | Frequency modulation |
| FSK | = | Frequency shift keying |
| IF | = | Intermediate frequency |
| ISI | = | Intersymbol interference |

| | | |
|--------|---|---|
| LD | = | Laser diode |
| LED | = | Light emitting diode |
| LW | = | Linewidth |
| MSK | = | Minimum shift keying |
| MSK-FM | = | FM with MSK subcarrier |
| NRZ | = | Non-return to zero |
| OOK | = | On-off keying |
| OFDM | = | Optical frequency division multiplexing |
| PDF | = | Probability density function |
| PIN | = | Positive intrinsic negative |
| PRBS | = | Pseudorandom bit sequence |
| PSK | = | Phase shift keying |
| SNR | = | Signal-to-noise ratio |

LIST OF FIGURES

| | | |
|----------|--|----|
| Fig. 1.1 | Fundamental elements of communication system | 2 |
| Fig. 1.2 | Spectrum of electromagnetic waves | 2 |
| Fig. 1.3 | Block diagram of optical communication system. | 4 |
| Fig. 2.1 | Frequency modulation (FM) response of a practical distributed feedback (DFB) laser. | 16 |
| Fig. 2.2 | Impulse response $m(t)$ corresponding to non-uniform FM response $M(f)$ of a DFB laser shown in fig. 2.1. | 17 |
| Fig. 2.3 | Block diagram of an optical heterodyne receiver with delay-demodulation. | 23 |
| Fig. 2.4 | Tabular and state diagram of Alternate-Mark-Inversion (AMI) linecoding. | 36 |
| Fig. 2.5 | Block diagram of an optical transmitter with linecoder | 36 |
| Fig. 2.6 | Effective pulse shape for NRZ data | 39 |
| Fig. 2.7 | Effective pulse shape for AMI encoded data | 40 |
| Fig. 2.8 | The average phase error vs. modulation index for NRZ data. | 41 |

| | | |
|------------------|--|-----|
| Fig. 2.9 | The average phase error vs. modulation index for AMI data. | 42 |
| Fig. 2.10 | Probability density function of phase error vs. θ for $h=0.83$ | 44 |
| Fig. 2.11 | Probability density function of phase error vs. θ for $h=0.83$) | 45 |
| Fig. 2.12 | Bit error rate performance of optical CPFSK system with delay-demodulation for NRZ and AMI coded data with $\Delta\nu T = 0.0$ | 46 |
| Fig. 2.13 | Bit error rate performance of optical CPFSK system with delay-demodulation for NRZ and AMI coded data with $\Delta\nu T = 10^{-3}$ | 47 |
| Fig. 2.14 | Bit error rate performance of optical CPFSK system with delay-demodulation for NRZ and AMI coded data with $\Delta\nu T = 0.0 \& 10^{-3}$.48. | |
| Fig. 2.15 | Bit error rate performance of optical CPFSK system with delay-demodulation with NRZ and AMI coded data for several values of modulation index and normalized linewidth | 50 |
| Fig. 2.16 | Power penalty vs. normalized linewidth for several values of modulation index with AMI encoded data | 51. |

| | | |
|------------------|---|-----|
| Fig. 2.17 | Power penalty vs. modulation index for several values of normalized linewidth. | 52 |
| Fig. 2.18 | Comparison of theoretical BER results with those of published paper. | 54 |
| Fig. 3.1 | The original pdf $f_X(x)$ and the transformed pdf $g_X(x)$ | 58 |
| Fig. 3.2 | IF frequency deviation with non-uniform LD FM response | |
| | (a) for NRZ data | 66 |
| | (b) for AMI encoded data | 67 |
| Fig. 3.3 | Comparison of theoretical and simulation results for bit error rate of optical CPFSK system with $\Delta\nu T = 0.0$ | 69 |
| Fig. 3.4 | Comparison of theoretical and simulation results for bit error rate of optical CPFSK system with AMI coded data for several values of linewidth with modulation index $h=0.9$ | 70 |
| Fig. A.1 | Flow chart for computer simulation of optical heterodyne CPFSK system with delay-demodulation | A.1 |

ABSTRACT

In coherent optical communication system, continuous phase frequency shift keying (CPFSK) modulation of distributed feedback laser diode (DFB-LD) is the most attractive scheme due to direct frequency modulation capability of DFB-LD, high receiver sensitivity, compact IF spectrum and high fibre-launched power. In this work, a theoretical formulation is developed to evaluate the degrading effect of non-uniform FM response of DFB-LD on the performance of optical heterodyne CPFSK receiver with delay-demodulation in the presence of receiver noise and laser phase noise due to non-zero laser linewidth. The effectiveness of Alternate-Mark-Inversion (AMI) linecoding in counteracting the the effect of non-uniform LD FM response is also investigated.

The optical CPFSK system suffers a bit error rate floor due to the non-uniform LD FM characteristic. With non-return to zero (NRZ) data, the error rate floor occurs at much higher values and the desired error rate performance at an error rate of 10^{-9} can never be achieved. When the AMI linecoding is employed, there is a significant reduction in the bit error rate floor. The performance can be further improved by increasing modulation index and the system suffers a minimum penalty of 2.05 dB at BER= 10^{-9} with $\Delta\nu T = 10^{-4}$ at an optimum modulation index of 0.9. Further increase in modulation index causes the penalty to increase further. The optimum values of modulation index are slightly higher for larger values of linewidth.

Finally, a statistical Monte-Carlo simulation technique using 'importance sampling' is employed to estimate the performance of the CPFSK delay-demodulation receiver. The theoretical results are well confirmed by the simulation results and the experimental results reported earlier.

CHAPTER 1



INTRODUCTION

1.1 Communication System

From the very beginning of civilization, the human trend has been to devise communication systems for sending messages from one distant place to another. Such a communication system has the following fundamental elements, as shown in figure 1.1,

i) an information source, which produces an information signal carrying the message to be sent,

ii) a transmitter, which couples the information onto a transmission channel in the form which matches the transfer properties of the channel,

iii) a transmission medium or channel, which bridges the distance between transmitter and receiver,

iv) a receiver, which extracts the desired signal from the channel, amplifies it and restores it to its original form before passing it to the message destination.

The motivations behind communication research are to improve the transmission fidelity, to increase the data rate so that more information can be sent, and to increase the transmission distance between relay stations. Many forms of communication systems have been devised. Earlier communication systems were of a very low data rate and basically involved only optical transmission links, for example, was the use of a fire signal. In the fourth century B.C., the transmission distance was extended through the use of relay stations. By 150 B.C., the optical signals were encoded in relation to the alphabet so that any message could be sent.

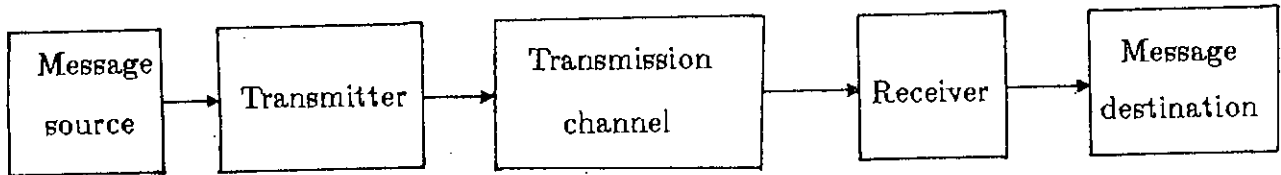


Figure 1.1: Fundamental elements of communication system.

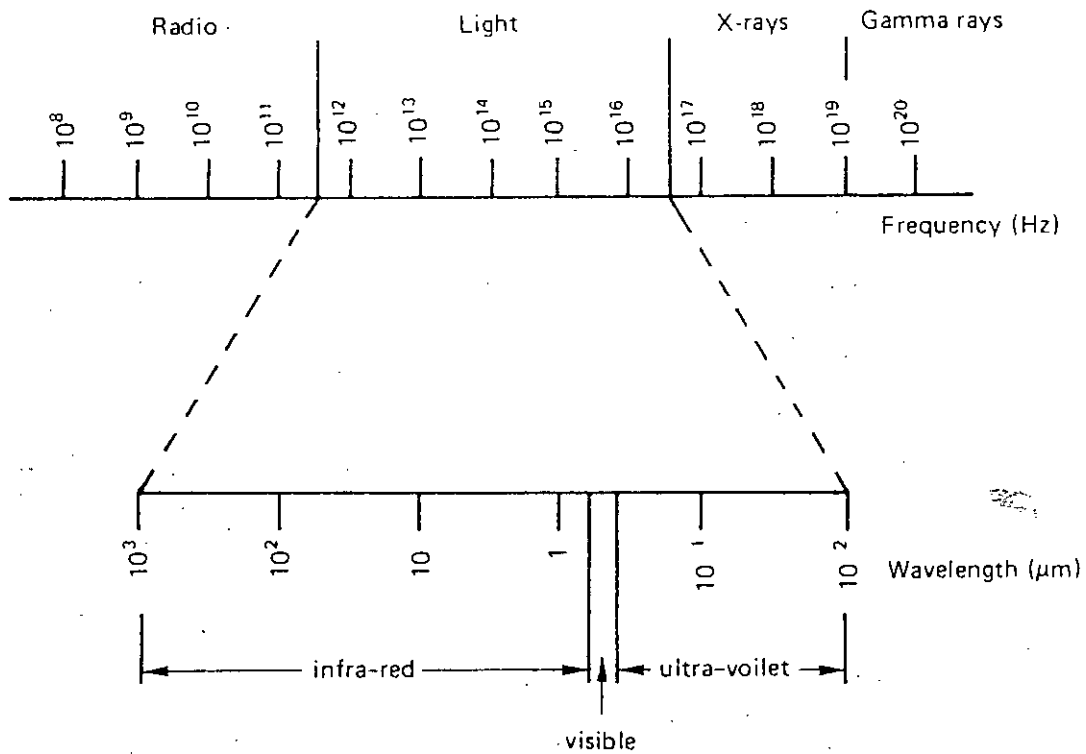


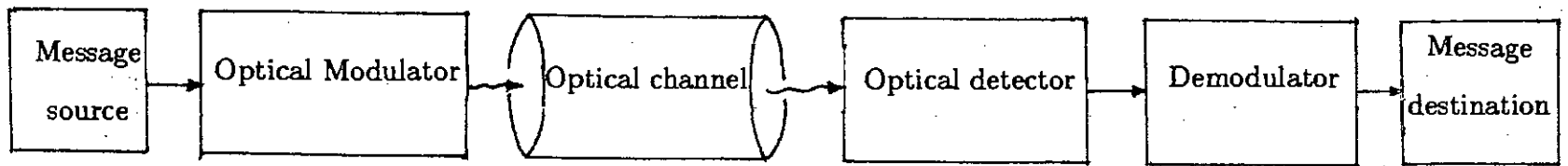
Figure 1.2: Spectrum of electromagnetic waves.

The discovery of telegraph made a revolution in communication and electrical communication then was realized. Wire cable was the only medium for electrical communication until the discovery of long wavelength electromagnetic radiation in 1887. Message is usually transferred over the channel by superimposing the information signal onto a sinusoidally varying electromagnetic wave known as carrier. The amount of information that can be transmitted is directly related to the frequency range over which the carrier wave operates. Therefore, the trend in electrical communication development has been to employ progressively higher frequencies (shorter wavelengths) which offers corresponding increase in bandwidth, and hence, an increased information capacity. This activity led, in turn, to the invention of television, radar and microwave links.

1.2 Optical Communication

An important portion of the electromagnetic spectrum is the optical region which is $50nm - 100\mu m$. The desire for reliable and economical transmission with large information capacity has shown a great interest to employ these optical frequencies for communication. When the laser was first realized in 1960, its potential usefulness as a coherent source for optical transmission was immediately recognized, and work in optical communications begin in earnest [1]. At first lightwave propagation through the atmosphere and through periodic focusing elements in a controlled environment were studied both theoretically and experimentally. Experimental line-of-sight atmospheric systems were demonstrated, but the reliability and hence, the usefulness of such systems were shown to be limited by adverse weather conditions [1].

The first proposal to employ the optical fiber as a transmission medium appeared in 1966. Initially the loss in optical fiber was extremely large, about 1000 dB/km at $\lambda = 0.82\mu m$ [1]. Gradually the transmission losses in fiber are reduced and also the reliability of semiconductor injection lasers is improved. The optical loss in fiber in now-a-days is as low as 0.47 dB/km at $\lambda = 1.2\mu m$ [1].



4

Figure 1.3: Block diagram of optical communication system.

The principal advantage of optical communication is the potential increase in information and power that can be transmitted. Since optical frequencies are of the order of 10^{14} Hz, optical communication has a theoretical information capacity exceeding that of microwave systems by a factor of 10^5 . In addition, the ability to concentrate available transmitted power within the transmitted electromagnetic wave also increases with increase in the carrier frequency. Thus the use of optical frequencies increases the capability of the system to achieve higher power densities, which generally leads to improved performance.

Another important advantage of optical communication is the dielectric nature of optical fibres which provides immunity to electromagnetic interference. The freedom from ground-loop problems, very low fibre-to-fibre cross talk, the small size of individual fibre and the allowable small bending radius of fibre cable are some of the other features which make optical fiber communication attractive. An additional importance is the advantage that silica is the principal material for optical fibers, which is abundant and inexpensive as its main source is sand.

However, optical communication has several difficulties. Since optical frequencies have extremely small wavelengths, optical component design is more sophisticated than that of radio or microwave devices. A significant advance was made by the advent of laser as a relatively high-powered optical carrier source. Further progress was made by the development of wideband optical modulators and efficient detectors.

Another drawback of optical communication is the effect of the propagation path on the optical carrier wave. This is because optical wavelengths are commensurate with molecule and particle sizes, and propagation effects are generated that are uncommon to radio and microwave frequencies. Furthermore, these effects tend to be stochastic and time-varying in nature, which hinders accurate propagation modeling.

1.2.1 Optical Sources

The optical source converts the electrical information signal into optical signal. The principal light sources used in optical communication are light-emitting diode (LED) and laser diode (LD). For systems requiring bit rates less than approximately 50 Mb/s together with multi-mode fibre-coupled optical power in the tens of microwatts, semiconductor LEDs are usually the best light source [2]. LEDs require less complex drive circuitry than LDs since no thermal or optical stabilization circuits are needed and they can be fabricated less expensively with higher yields. But the optical output from an LED is incoherent. There exists no optical cavity for wavelength selectivity. The output radiation has a broad spectral width since the emitted photon energies range over the energy distribution of the recombining electrons and holes which lie between 1 and $2kT$ [2]. In addition, the incoherent optical energy is emitted into a hemisphere according to a cosine power distribution and, thus, has a large beam divergence.

On the other hand, the optical output from an LD is coherent. The optical energy is produced in an optical resonant cavity. This optical signal has spatial and temporal coherence, which means that it is highly monochromatic and the output beam is very directional. These devices are suitable for fibre transmission systems because

- i) they have adequate output power for a wide range of applications,
- ii) the optical signal output can be directly modulated by varying the input current to the device,
- iii) they have a high emission efficiency, and
- iv) their dimensional characteristics are compatible with those of the optical fibre.

In choosing an optical source compatible with the optical waveguide, various characteristics of the fibre such as its geometry, its attenuation as a function of wavelength, its group delay distortion (bandwidth), and its modal characteristics must be taken into

account. The interplay of these factors with the optical source power, spectral width, radiation pattern and modulation capability needs to be considered.

1.2.2 Optical Detectors

The device at the receiving end of optical fibre which interprets the information contained in the optical signal is the photodetector. The photodetector senses the luminous power falling upon it and converts the optical signal to a corresponding electric current. Since the optical signal is generally weakened and distorted when it emerges from the end of the fibre, the photodetector must meet very high performance requirements. It should have high sensitivity in the emission wavelength range of the optical source being used, a minimum addition of noise to the system, and a fast response speed or sufficient bandwidth to handle the desired data rate. It should also be insensitive to temperature variations and be compatible with the physical dimensions of the optical fiber.

Several types of photodetectors are available, photomultipliers, pyroelectric detectors, and semiconductor-based photoconductors, phototransistors and photodiodes. Semiconductor-based photodetectors meet the requirements of optical detectors. Among them, photodiode is used almost exclusively for optical fiber communication because of its small size, suitable material, high sensitivity and fast response time. The two types of photodiodes used are the *pin* photodetector and the avalanche photodiode (APD). Avalanche photodiodes are more useful because they internally multiply the primary signal photocurrent before it enters the input circuitry of the following amplifier. This increases receiver sensitivity since the photocurrent is multiplied before encountering the thermal noise associated with the receiver circuit.

1.2.3 Detection Schemes

In optical communication system, two important detection strategies are normally employed, viz., direct detection and coherent detection. In a direct detection reception, the intensity of the received optical field is directly converted to a current by a photodetector. In coherent detection, the received optical field is combined with the light output from a local oscillator laser and the mixed optical field is converted to an IF signal by heterodyning or directly to a baseband by homodyning. The direct detection optical systems used in terrestrial communication are well matured. However, there are sufficient scopes of more investigations in space borne direct detection systems.

Heterodyne detection system suffers 10-20 dB performance improvement over direct detection system because of the use of local oscillator. Significant progress has been made on coherent optical systems during the last decade and it has become more than just a promise for future applications. Although some technical and financial difficulties have still to be completely overcome before coherent systems become of common use, field trials have begun to be successfully reported upon by the most important industries in the world for long-haul (point-to-point) transmission and also for multi-channel applications [3].

1.2.4 Modulation schemes

Digital information can be impressed upon a carrier wave in many ways. The basic types are amplitude shift keying (ASK), frequency shift keying (FSK) and phase shift keying (PSK). Given a digital message, the simplest modulation technique is ASK, wherein the carrier amplitude is switched between two or more values. In optical communication, a common form of ASK is on-off keying (OOK), used for binary information signals. The modulated wave consists of optical pulses or marks, representing binary 1, and no pulses or spaces, representing binary 0. Similarly, in FSK, the optical carrier frequency is switched between different frequencies corresponding to different informa-

tion. With binary information signal, the carrier frequency is f_1 for binary 1 and f_0 for binary 0. In PSK, the phase of the carrier is keyed in a similar way.

In optical communication, FSK systems are more promising than ASK or PSK, because [4]

i) modulation can be easily performed using direct frequency modulation capability of laser diode (LD) modulation,

ii) direct FSK modulation gives large transmitting power without external modulator loss,

iii) distributed feedback (DFB) LDs without external cavities achieve stable operation,

iv) optical frequency division multiplexing is possible.

Demodulation of optical heterodyne FSK can be achieved by single-filter, dual-filter and discriminator demodulation. The type of intermediate frequency (IF) demodulation used in an optical FSK receiver is determined by the IF linewidth, the available receiver bandwidth and the degree of complexity that one is willing to accept. Both frequency discriminator and dual-filter detection techniques provide comparable performance for large deviation FSK. However, when FSK signaling desired with broader linewidth lasers, both larger frequency deviation and wider IF bandwidths are necessary for dual-filter detection to ensure optimum receiver performance. With large IF bandwidth, the frequency squared receiver noise component is very large and the design of wideband receivers is complicated. Further, the implementation of of a wideband receiver at high bit rates is difficult in practice. For these reasons, FSK receiver with large deviation which retains only a single IF filter centred at the 'mark' frequency is preferred. This will require less bandwidth with 3 dB less sensitivity compared to FSK dual-filter detection.

Among FSK schemes, continuous phase FSK (CPFSK) scheme has attracted much

interest in recent years because of its high receiver sensitivity and compact IF spectrum [4]. Coherent optical transmission using CPFSK heterodyne delay-demodulation is being considered seriously for operational use because the receiver sensitivity can be within 3.5 to 5 dB of the most sensitive coherent system, and no optical phase-locked loop is needed [3].

1.3 Brief Review of Previous Works

To achieve high receiver sensitivity using CPFSK coherent detection, there are a number of problems to be solved. The performance of an optical heterodyne receiver can be severely degraded by

- i) the non-uniform frequency modulation (FM) response characteristics of DFB lasers, and
- ii) the phase noise of the transmitting and LO lasers,
- iii) the intensity fluctuations of the receiver's local oscillator (LO),
- iv) the photodetector shot noise and receiver thermal noise,
- v) the transmission medium limitations, such as the polarization problems in a coherent transmission system.

Intensity fluctuation of LO laser produces excess noise at the photodetector output and the receiver performance degradation due to intensity noise can be substantial (0-40dB) [3]. The excess noise can be reduced by a (balanced photodetector) dual-detector receiver.

The detection performance of a coherent lightwave transmission link can be sharply degraded by laser phase noise. The phase noise of LD's is due to the non-zero spectral linewidth. Generally the linewidth of conventional DFB/DBR LD is about 10MHz [4]. In the absence of phase noise, the best way to detect the intermediate frequency

(IF) signal would be to extract a carrier reference from it and then perform coherent demodulation to baseband. But the random phase can have large and rapid variations. The finite IF linewidth of the sources is a measure of the phase noise acting and the effect of phase noise is more critical in the case of phase coherent signaling like PSK, DPSK and CPFSK but comparatively less significant in the case of noncoherent ASK and PSK signaling [5]. The effect of laser phase noise on the performance of digital coherent optical communication systems has been the subject of considerable theoretical study [5-16]. Some experiments have also been reported which have investigated the effect [10]. When the IF linewidth β is very much smaller than the data rate, it is often sufficient in a bit error rate analysis to assume that the IF phase is constant during the bit period T but the IF phase varies randomly from one bit period to another. Several analysis of moderately coherent systems such as CPFSK [9,13-15] have been performed on this basis.

The performance of FSK systems depend largely upon the device characteristics of the semiconductor lasers. The conventional DFB lasers have a dip in the FM response characteristic in several MHz region. The non-flat FM response results in continuous drift in the frequency of the transmitted FSK tones which can severely degrade the overall system performance by spreading the tone energy over a wide bandwidth, thereby, increasing the crosstalk between tone-slots. The error rate performance of the system exhibits bit error rate (BER) floors for long pseudo-random data pattern [4]. To overcome the effect of non-uniform FM response of DFB lasers, several techniques have been suggested in practice, viz., use of multi-electrode DFB lasers [18], passive equalization of FM characteristics using compensation circuitry [19], direct modulation of phase tunable lasers [20], adaptive quantized feedback equalization in the receiver [21], the use of line coding for the laser driving signal [22-24] and the use of subcarrier modulation with analog optical FM such as MSK-FM [48]. Recently, performance degradation of optical heterodyne FSK with single-filter (envelope detection) receiver due to non-flat FM response is reported for non-return to zero (NRZ and linecoded data pattern [3].

However, no theoretical predictions or simulation results are yet available which account for the performance degradation of optical FSK heterodyne delay-demodulation receiver caused by the the combined effect of the receiver noise, phase noise and the non-uniformity in FM response of DFB lasers.

Optical heterodyne receivers attain maximum detection sensitivity when the polarization states of the signal and reference light waves coincide. Several countermeasures have also been proposed in the literature [25] to handle the signal fading due to polarization mismatch in coherent communication systems.

1.4 Objective of the Thesis

The objective of the is to study the degrading effect of non-uniform frequency modulation (FM) characteristics of distributed feedback laser diode (DFB-LD) on the performance of an optical CPFSK heterodyne delay demodulation system. A theoretical formulation is developed to evaluate the performance of the receiver under the combined influence of non-uniform FM response of the lasers, laser phase noise and receiver noise.

The theoretical analysis is extended to study the effectiveness of Alternate-Mark-Inversion (AMI) linecoding in overcoming the effect of non-uniform FM response of lasers.

A statistical Mote-Carlo simulation of the system is carried out. In the computer simulation the 'composite importance sampling' technique is employed for generation of noise samples at the tail region of the pdf curve.

1.5 Organization of the Thesis

In chapter 1, a brief introduction to optical communication is presented. The major features of optical communication system are discussed in brief. A review of recent works in the related field is also presented in the discussion.

In chapter 2, the performance of coherent optical heterodyne CPFSK delay-demodulation system is analyzed. The limitations are discussed in brief. Theoretical formulation is developed to evaluate the bit error performance of the system taking into account the effect receiver noise, laser phase noise and non-uniform FM response of laser. The AMI linecoding is included in the analysis to study its effectiveness in reducing the effect of pattern dependent modulation.

In chapter 3, a method is presented to simulate the coherent optical heterodyne CPFSK delay-demodulation system with the help of digital computer. The performance of the system is evaluated by computer simulation and the results are compared with the theoretical evaluation. The importance sampling technique is employed in the simulation.

In chapter 4, concluding remarks on this work are presented. In addition, some recommendations for further work are presented.

CHAPTER 2

OPTICAL CPFSK HETERODYNE RECEIVER WITH DELAY-DEMODULATION

2.1 Introduction

Coherent optical communication systems become attractive with recent great advances in devices and several relevant controlling technologies for optical frequency and polarization. To apply coherent technology to practical systems, it is necessary to operate a system stably. In regard to stability or practicability, frequency-shift-keying (FSK) systems with distributed feedback laser diode (DFB-LD) are most useful. Because a direct FSK modulation gives large transmitting power without external modulator loss, and DFB-LDs without external cavity achieve stable operation. Among FSK systems, the continuous-phase frequency-shift-keying (CPFSK) optical heterodyne delay-demodulation system seems to be the most attractive, because of its high fibre-launched power, high receiver sensitivity and compact IF spectrum [4,27]. With this modulation found, however, a serious problem arises owing to the non-uniform frequency modulation (FM) response [4,26] of the conventional DFB-LDs which causes the system performance to be data pattern dependent.

In this chapter, a detailed theoretical analysis is provided to evaluate the effect of non-flat FM response of DFB-LD on the performance of optical heterodyne CPFSK system with delay-demodulation. The analysis is carried out in the presence of laser phase noise and additive receiver noise. The analysis is extended to Alternate-Mark-

Inversion (AMI) linecoded CPFSK system to evaluate the effectiveness of linecoding in counteracting the degrading effect of non-flat FM response.

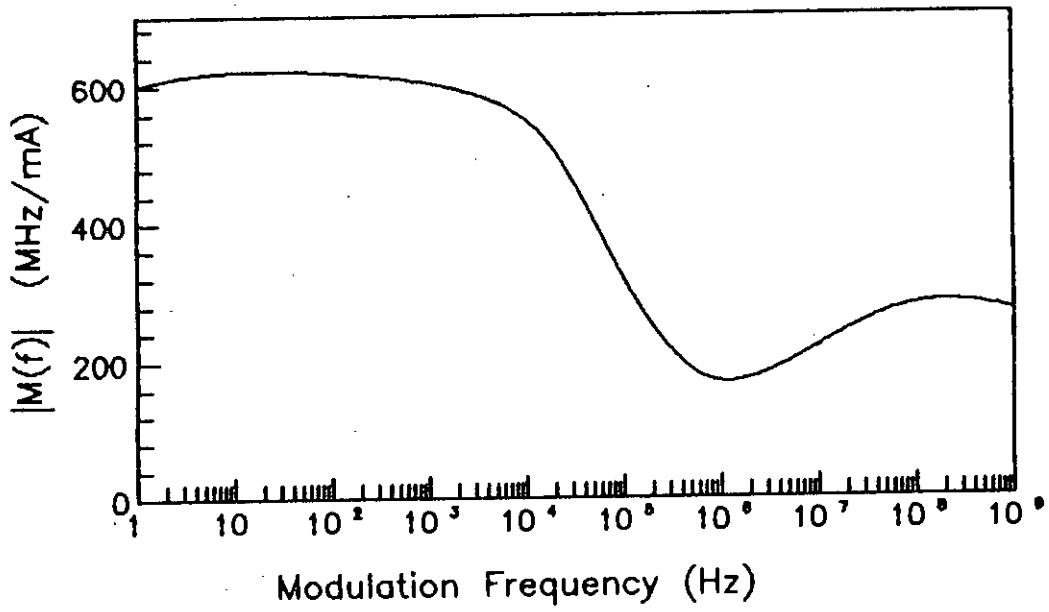
2.2 Performance Limitations

The performance of a coherent optical heterodyne CPFSK delay-demodulation system is degraded by a number of problems. The major problem is the non-uniformity in the frequency modulation (FM) characteristics of semiconductor laser diodes. The another important problem is the phase noise arising due to the nonzero spectral linewidth of DFB-LD output. Besides, the shot noise produced in the process of photodetection and thermal noise introduced by the receiver circuitry cause degradation of receiver performance. The polarization mismatch between the signal and the reference lightwave is an additional problem in optical heterodyne receiver.

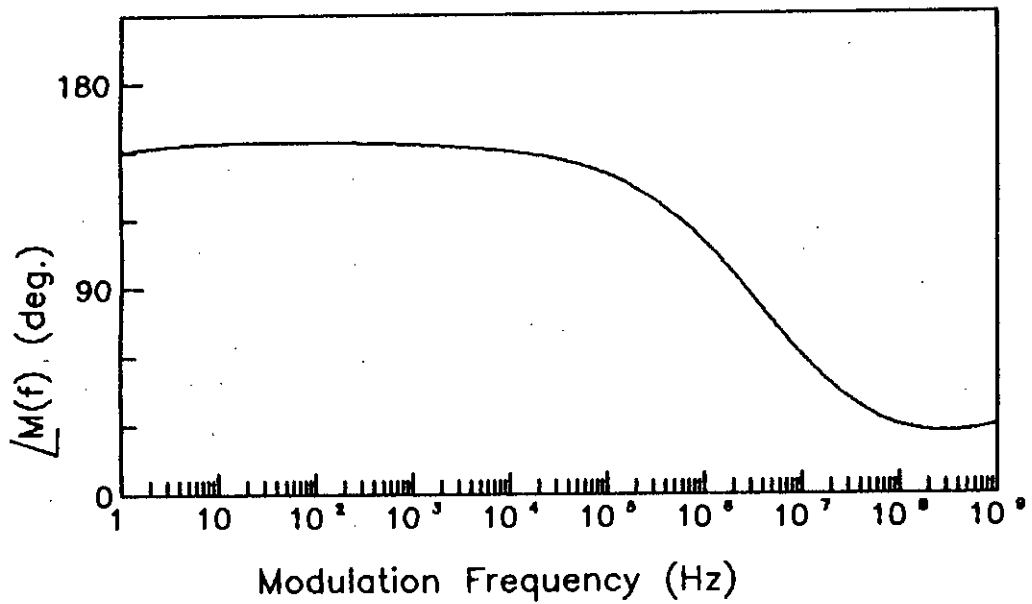
2.2.1 Non-uniform FM Response of Laser

The direct frequency modulation capability of a semiconductor laser through an injection current modulation [26] is promising for the applications to the coherent transmission system, since an FM transmitter and a tunable local oscillator can be realized with a conventional semiconductor laser. A large frequency shift by a small modulation current without serious unintended intensity modulation is desired for the above applications.

The generation of CPFSK optical signals is easily achieved by modulating the injection current of a semiconductor distributed feedback laser diode (DFB-LD). A change of this bias current determines a change of both the carrier density and the temperature of the laser active layer. A carrier density change in the active layer results in a refractive index change through both the free carrier plasma dispersion and anomalous dispersion. An increase in the carrier density brings about a decreased refractive index and increases the oscillation frequency. In a low-modulation frequency region, the active



(a)



(b)

Figure 2.1: Frequency modulation (FM) response of a practical distributed feedback (DFB) laser

(a) amplitude,

(b) phase.

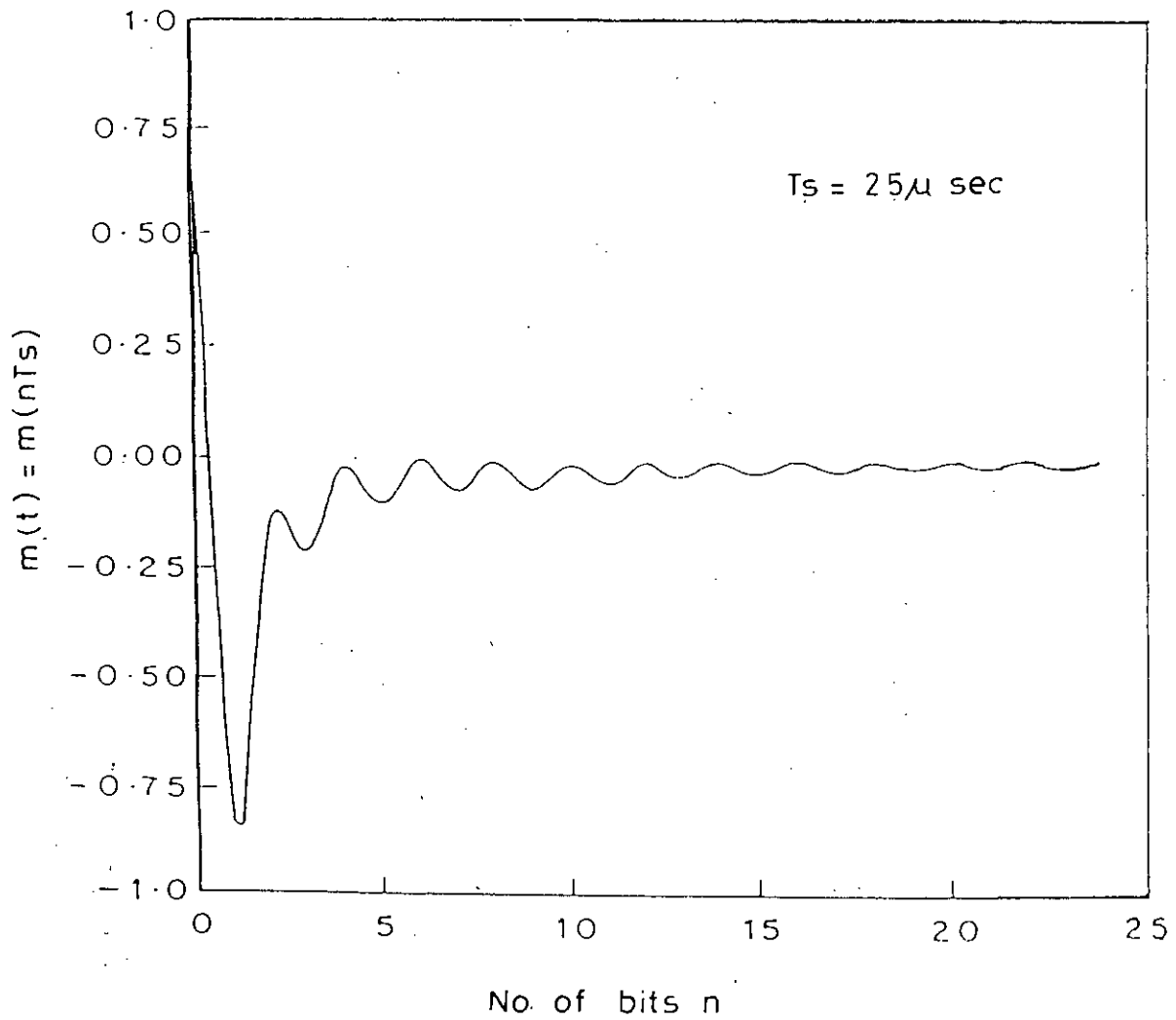


Figure 2.2: Impulse response $m(t)$ corresponding to non-uniform FM response $M(f)$ of a DFB laser shown in fig. 2.1.

layer temperature change follows the injection current modulation. Thermal expansion of the active layer and a thermal increase in the refractive index result in a decreased oscillation frequency.

An ideal laser would exhibit flat FM response corresponding to a constant frequency deviation per unit current deviation for any modulation frequency. Then the impulse response of the laser would be $m(t) = -\Delta f \delta(t)$ corresponding to the transmitted bit '1', where $\delta(t)$ is a delta dirac function and Δf is the peak frequency deviations.

However, in a practical DFB laser, frequency modulation is highly dependent on the modulation frequency of the bias current. A nonideal laser exhibits non-uniform FM response along with phase distortion. Hence the impulse response of a DFB laser, instead of being a delta function, have finite duration in time introducing the pattern dependent modulation effect. The FM response and impulse response of a typical DFB laser is shown in figures 2.1 and 2.2 respectively.

The non-uniform modulation characteristics are due to the co-existence of the fast responding carrier density modulation effect and the slow responding temperature modulation effect in the active layer. The change in the refractive index due to the carrier density change is fast, but at low modulation frequencies the temperature sweep due to the bias current produces a refractive index change that is opposite to the carrier effect. Also the carrier density modulation does not have so large effect comparable to the temperature change, because the lasing clamps the carrier level tightly in the active layer. However, the relaxation oscillation brings large effect in the high frequency region. As a result, DFB-LDs show a dip in its FM characteristics (between 0.1 and 100MHz) and the non-uniform FM response arises [24].

Nonideal FM characteristics including the amplitude and phase distortion, results in continuous drifts in the frequency of the transmitted FSK tones. Tone frequency drift can severely degrade the overall performance by spreading the tone energy over a wide bandwidth, thereby increasing the cross-talk between tone slots. A floor in the

bit error rate (BER) characteristic of the system is experienced for long pseudo-random data patterns [3,4].

Several countermeasures to the effect of non-uniform FM characteristic of DFB lasers are possible at both device and system level. These are

- i) use of multi-electrode DFB laser [18],
- ii) passive equalization of FM characteristic using compensating circuitry [19],
- iii) appropriate line coding for the laser driving signal [22-24],
- iv) use of subcarrier modulation with analog optical FM, such as MSK-FM [48],
- v) direct modulation of phase tunable laser [20] and
- vi) adaptive quantized feedback equalization at the receiver [21].

2.2.2 Laser Phase Noise

Though lasers are expected to be highly coherent, practical lasers are not. There is always a spectral linewidth associated with a laser output. That means, the laser oscillation is not of a single frequency, but also contains some side frequencies. Generally the linewidth obtained with conventional DFB/DBR-LD is about 10MHz [4]. These extra frequencies appear as phase noise in the laser output.

In a heterodyne optical receiver, in addition to the transmitting laser phase noise, the local oscillator also produces another phase noise. This heterodyning operation also adds signal shot noise. In the absence of phase noise, the best way to detect the IF signal would be to extract a carrier reference from it and then perform the coherent demodulation to the baseband. The problem with this approach when phase noise is present, is that the random phase can have large and rapid variations. Hence a carrier recovery circuit might track it so imperfectly as to seriously degrade the demodulation process and the follow-on data detection.

An alternate approach is to use IF envelope detection. For a bit error rate of 10^{-9} , envelope detection requires only about 0.5dB more signal power than does ideal coherent demodulation [7]. This result, however, applies to signals with no phase noise for which the optical IF filter is a matched filter with noise bandwidth $\frac{1}{T}$ (bit rate). In situations where the phase is randomly varying, significantly wider IF bandwidths are needed to pass the signal undistorted, and this has the effect of increasing the noise power at the output of the envelope detector. A useful practice is to offset this noise increase by following the envelope detector by a low pass filter.

In a coherent receiver, it is the phase noise which determines the limiting performance of the receiver. The finite IF linewidth of the source is a measure of the laser phase noise acting and whose effect is more critical in the case of phase coherent signaling like PSK, DPSK and CPFSK, but comparatively less significant in the case of noncoherent ASK and FSK signaling. For large values of the source linewidth (or equivalently IF linewidth), the latter systems experience limiting performance in the form of BER floors which can not be lowered even by increasing the local oscillator power. The position of the floor depends on the laser linewidth, the modulation index and the IF bandwidth. The error rate floor can be lowered by increasing the value of the modulation index, choosing better lasers having low values of linewidth or incorporating some coding techniques.

The CPFSK delay demodulation system requires a higher spectral purity compared with noncoherent detection systems. A general approach to achieving the CPFSK delay demodulation system is to use narrow spectral width light sources such as external cavity lasers. However from a practical point of view, it is desirable to use standard LDs without external cavities. To achieve the CPFSK delay-demodulation system using DFB-LDs with more than 10MHz IF beat spectral width, it is necessary to adopt a large modulation index to avoid LD phase noise influence [27]. With the modulation index increment, the IF spectrum is broadened and the required IF bandwidth becomes large.

In this case, an increase in the IF noise degrades the receiver sensitivity.

2.2.3 Local Oscillator Excess Noise

The performance of a single detector optical heterodyne receiver can be degraded by intensity fluctuations of the receiver's local oscillator. Such fluctuations produce a noise at the detector photocurrent in excess of the usual quantum shot noise. If the excess photocurrent noise is comparable to or larger than the quantum shot noise, receiver performance may be degraded. For noisy local oscillator lasers, receiver performance degradation due to intensity noise can be substantial (2-40dB) [3].

The cancellation of excess noise can be effected by a double-detector receiver [28]. A received optical beam is mixed with a local oscillator beam by means of a beam splitter/fibre directional coupler acting as 180 degree hybrid [3]. At the detectors the mixed fields produce two photocurrents each of which includes the beat signal and the additive noise. The detector outputs are then fed into a difference amplifier. Since there is a phase difference of 180 degree between the beat signals in the two photocurrents, the two beat signals will add constructively at the output of the difference amplifier whereas the in-phase local oscillator intensity noise components of the two photocurrents will tend to cancel.

2.2.4 Receiver Noise

During photodetection process, shot noise arises which is due to the random production and collection of photons. Also thermal noise arises in the receiver passive circuit. The total receiver noise is modelled as additive white Gaussian noise (AWGN).

2.2.5 Polarization Problems

Optical heterodyne receivers attain maximum detection sensitivity when the polarization states of the signal and reference lightwaves coincide. The polarization mismatch between signal and reference lightwaves causes deterioration of detection efficiency. In addition, polarization fluctuation of the signal lightwave causes signal-dependent noise (polarization noise) which deteriorates the carrier-to-noise ratio (CNR) of the IF signal significantly. There is approximately 10dB degradation in the CNR of an IF signal obtained by heterodyne detection when a polarization fluctuation as small as 0.1π radian exists [3].

2.3 Receiver Model

The model of an optical heterodyne delay-demodulation receiver is shown in figure 2.3. The light source used by the transmitter is assumed to be a single-mode laser, and the receiver includes a similar laser used as a local oscillator (LO). The received optical signal is mixed with the LO signal. The combined optical signal is detected by a photodetector and thus a microwave intermediate frequency (IF) electrical signal is produced. During the conversion process, Gaussian noise is added in two ways,

- 1) shot noise produced in the process of photodetection, and
- 2) thermal noise introduced by the circuitry following the photodetector.

The IF signal at the output of photodetector is filtered by a bandpass IF filter centered at the IF frequency. In absence of laser phase noise and with ideal LD FM response, the optical IF filter would be a matched filter with integration time equal to bit period [7]. With phase noise present, a shorter integration time and hence a larger IF bandwidth ($B_{IF} > \frac{1}{T}$) is required in situation experiencing non-zero IF linewidth and/or nonflat LD FM response [7].

After IF filtering, demodulation is performed by delay-demodulation technique. The

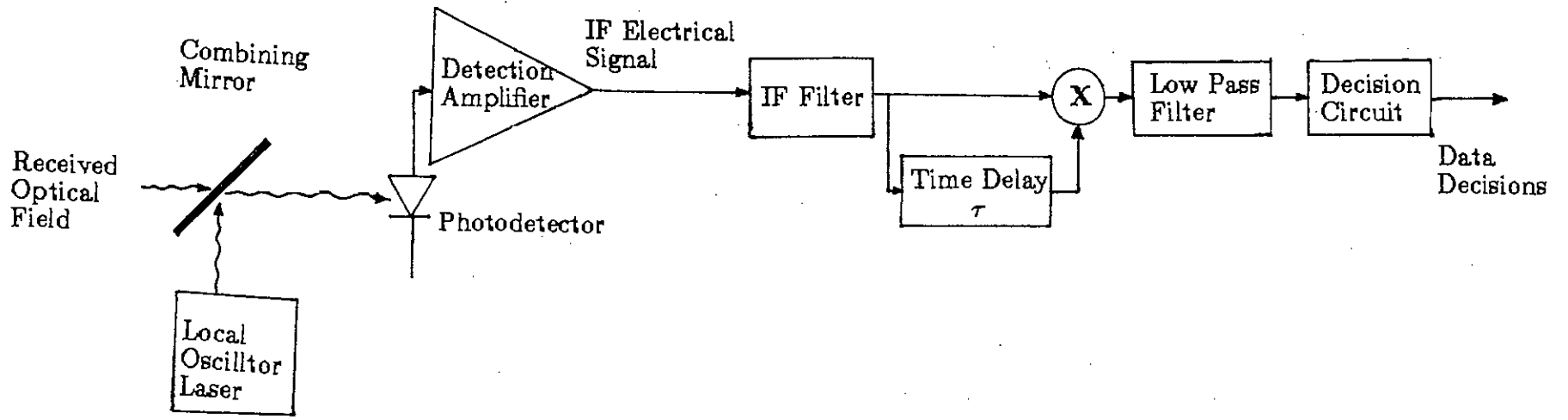


Figure 2.3: Block diagram of an optical heterodyne receiver with delay-demodulation.

signal and its time-delayed (by τ) version are multiplied. With certain conditions maintained, the polarity of the output signal, after passing through a low pass filter, contains the bit information. Data decision is made by using the polarity of this output signal.

2.4 Theoretical Analysis

2.4.1 The Optical Signal

The optical signal with carrier frequency ω_c and power P_S , received at the receiver front end, can be expressed by

$$s(t) = A_s \cos[\omega_c t + \phi_s(t) + \phi_{nT}(t)] \quad (2.1)$$

where

$P_s = \frac{A_s^2}{2}$, for normalized impedance $|Z| = 1$.

So,

$$s(t) = \sqrt{2P_S} \cos[\omega_c t + \phi_s(t) + \phi_{nT}(t)] \quad (2.2)$$

where,

$\phi_s(t)$ = angle modulation

$\phi_{nT}(t)$ = phase noise of transmitting laser.

The angle modulation can be written as

$$\phi_s(t) = 2\pi \int_{-\infty}^t I(t) * m(t) dt \quad (2.3)$$

where,

$I(t)$ = NRZ information bit sequence given by,

$$I(t) = \sum_{n=-\infty}^{\infty} a_n p(t - nT) \quad (2.4)$$

a_n = nth information bit = ± 1

$m(t)$ = impulse response of transmitting laser corresponding to the normalized version of the FM response characteristics, $m(t) = F^{-1}[M(f)]$

So, we can write

$$\begin{aligned}
\phi_s(t) &= 2\pi \int_{-\infty}^t \sum_{-\infty}^{\infty} a_n p(t - nT) * m(t) dt \\
&= 2\pi \int_{-\infty}^t \sum_{-\infty}^{\infty} a_n p'(t - nT) dt
\end{aligned} \tag{2.5}$$

where,

$$p'(t) = p(t) * m(t).$$

The local oscillator generates an optical signal with power P_{LO} , as

$$s_{LO}(t) = \sqrt{2P_{LO}} \cos[\omega_{LO}t + \phi_{LO}(t)] \tag{2.6}$$

where ϕ_{LO} is the phase noise introduced by the local oscillator. The local oscillator has a nominal frequency ω_{LO} differing from the optical carrier frequency ω_c by the IF frequency ω_{IF} , i.e. $\omega_{IF} = |\omega_c - \omega_{LO}|$. So, the heterodyning operation results in a signal with carrier frequency shifted to ω_{IF} .

This optical signal is photodetected by a balanced photodetector with responsivity R . Then the electrical current at the output of photodetector will be proportional to the input optical power, i.e.,

$$\begin{aligned}
r'(t) &= R[s(t) + s_{LO}(t)]^2 \\
&= R[P_s \cos\{2(\omega_c t + \phi_s(t) + \phi_{nT}(t))\} + P_{LO} \cos\{2(\omega_{LO}t + \phi_{LO}(t))\}] \\
&\quad + 2R\sqrt{P_s P_{LO}} \cos\{(\omega_c - \omega_{LO})t + \phi_s(t) + \phi_{nT}(t) - \phi_{LO}(t)\} \\
&\quad + 2R\sqrt{P_s P_{LO}} \cos\{(\omega_c + \omega_{LO})t + \phi_s(t) + \phi_{nT}(t) + \phi_{LO}(t)\} \\
&\quad + R[P_s + P_{LO}]
\end{aligned} \tag{2.7}$$

The high frequency terms are filtered out by the detection amplifier bandwidth. So the ultimate signal at the input to the IF filter is

$$r(t) = S \cos[2\pi f_{IF}t + \phi_s(t) + \phi_n(t)] + n(t) \tag{2.8}$$

where,

$$S = 2R\sqrt{P_s P_{LO}},$$

$\phi_n(t)$ = composite phase noise of the transmitting and LO lasers,

$n(t)$ = complex additive white Gaussian noise (AWGN) with one-sided spectral density N_o which consists of shot noise and thermal noise. The power spectral densities of these noise processes are

$$N_{shot} = 2eR\sqrt{P_s P_{LO}} \quad (2.9)$$

$$N_{thermal} = \frac{4kTF_e}{R_L} \quad (2.10)$$

where

F_e = noise figure of the amplifier,

R_L = amplifier load resistance.

2.4.2 Noise Processes $n(t)$ and $\phi_n(t)$

The noise $n(t)$ is modeled as a complex Gaussian white noise with one-sided spectral density N_o . The characterizing parameter for the additive white noise is the signal strength S^2 normalized by the noise power in a specified bandwidth. We define the IF signal-to-noise ratio (IF SNR) as the ratio of the signal power to the noise power in bandwidth equal to the transmission rate $\frac{1}{T}$, i.e. $\rho = S^2 T / N_o$.

The composite phase noise $\phi_n(t)$ is the difference between the independent phase variations $\phi_{nT}(t)$ and $\phi_{LO}(t)$ of the transmitting and receiving lasers respectively. An established model is that the associated radian frequencies $\phi_{nT}(t)$ and $\phi_{LO}(t)$ are white and Gaussian [7]. If the spectral densities of $\phi_{nT}(t)$ and $\phi_{LO}(t)$ are denoted by η_1 and η_2 respectively (rps^2/Hz) then the 3-dB linewidths for the laser sources are $\beta_1 = \eta_1/2\pi$ and $\beta_2 = \eta_2/2\pi$ Hz [7]. The spectral shapes are Lorentzian (or first order Butterworth) functions. Thus the IF output of the photodetector will have a random frequency variation $\phi_n(t) = \phi_{nT}(t) - \phi_{LO}(t)$, that is white and Gaussian with a spectral density of $(\eta_1 + \eta_2) rps^2/Hz$ resulting in a 3-dB linewidth $\beta = \beta_1 + \beta_2$ Hz.

Garrett and Jacobsen [13,29,30] modeled phase noise as a random intermediate frequency process which has a random IF frequency fluctuation $\delta f(t)$ about the centre frequency of the IF filter. With an assumption that the linear filtering terms dominate, the statistics of the bandpass filtered beat frequency fluctuation with Lorentzian power spectra has been theoretically shown to be Gaussian with variance $\beta B_e/2\pi$ where B_e is the effective IF filter bandwidth [30], given by

$$B_e = \frac{1}{2} \int_{-\infty}^{\infty} \left| \frac{H(f)}{H(0)} \right|^2 df \quad (2.11)$$

where $H(f)$ is the transfer function of the bandpass IF filter.

2.4.3 Output Phase of IF Filter

From equation (2.6) we get

$$r(t) = S \cos[2\pi f_{IF} t + \phi(t)] + n(t) \quad (2.12)$$

where $\phi(t) = \phi_s(t) + \phi_n(t)$.

The signal, contaminated by white noise, will be passed through a bandpass filter. The bandpass noise $n(t)$ can then be expressed as [31]

$$\begin{aligned} n(t) &= R_n(t) \cos[\omega_{IF} t + \phi(t)] \\ &= n_i(t) \cos[2\pi f_{IF} t + \phi(t)] - n_q(t) \sin[2\pi f_{IF} t + \phi(t)] \end{aligned} \quad (2.13)$$

So, the equation (2.8) can be rearranged as

$$\begin{aligned} r(t) &= X(t) \cos[2\pi f_{IF} t + \phi(t) + \zeta(t)] \\ &= X(t) \cos[2\pi f_{IF} t + \phi'(t)] \end{aligned} \quad (2.14)$$

where,

$$X(t) = \sqrt{(S + n_i)^2 + n_q^2}$$

$$\zeta(t) = \tan^{-1}\left(\frac{n_q}{S + n_i}\right)$$

We assume the IF filter to be ideal bandpass filter about f_{IF} with bandwidth $2B$, where B is the baseband bandwidth of the transmitted signal. The above is a realistic value for practical values of laser linewidths i.e. in the presence of phase noise, $\beta T = 2$ is a good practical choice [47].

The output of the IF filter will be

$$\begin{aligned}
u(t) &= r(t) * q(t) \\
&= \int_0^{\infty} q(\tau)r(t-\tau)d\tau \\
&= A(t) \cos[2\pi f_{IF}t + \psi(t)]
\end{aligned} \tag{2.15}$$

where $q(t)$ is the impulse response corresponding to the transfer function $Q(f)$ of the filter. The impulse response of the normalized equivalent baseband filter can be defined as

$$h(t) = \frac{q(t)}{Q(f_{IF})} e^{-j2\pi f_{IF}t} \tag{2.16}$$

$h(t)$ is complex if $Q(f)$ is not symmetrical around f_{IF} i.e. if the IF filter is asymmetric.

Bedrosian and Rice [32] showed that the output phase process can be expressed as

$$\psi(t) = \text{Re}[h(t) * \phi'(t)] + \sum_{n=2}^{\infty} \frac{1}{n!} \text{Im}[j^n f_n] \tag{2.17}$$

The first term represents linear filtering of the input phase $\phi'(t)$ and the summation represents various orders of distortion introduced by the filter. Assuming that the linear filtering term dominates, we get the output phase process relative to the carrier phase of the IF filter output, as

$$\begin{aligned}
\psi(t) &= h(t) * \phi'(t) \\
&= h(t) * \phi_s(t) + h(t) * \phi_n(t) + h(t) * \zeta(t) \\
&= h(t) * 2\pi \int_{-\infty}^t \sum_{-\infty}^{\infty} a_n p'(\lambda - nT) d\lambda + h(t) * \phi_n(t) + h(t) * \zeta(t) \\
&= 2\pi \int_{-\infty}^t \sum_{-\infty}^{\infty} a_n g(\lambda - nT) d\lambda + \alpha_n(t) + \theta_n(t)
\end{aligned} \tag{2.18}$$

where

$$g(t) = p'(t) * h(t) = p(t) * m(t) * h(t) \quad (2.19)$$

$$\alpha_n(t) = h(t) * \phi_n(t) \quad (2.20)$$

$$\theta_n(t) = h(t) * \zeta(y) \quad (2.21)$$

2.4.4 Delay-demodulation with uniform LD FM response

In the ideal CPFSK system with uniform FM response of laser, the IF signal can be expressed as

$$\begin{aligned} u(t) &= A \cos[2\pi f_{IF}t - 2\pi\Delta ft + \alpha(t)], \quad \text{mark} \\ &= A \cos[2\pi f_{IF}t + 2\pi\Delta ft + \alpha(t)], \quad \text{space} \end{aligned} \quad (2.22)$$

where

$$2\Delta f = hB$$

h =FSK modulation index

B =bit rate ($\frac{1}{T}$)

The output of the delay-demodulation circuit is

$$v(t) = u(t)u(t - \tau) \quad (2.23)$$

The delay time for the delay-demodulation circuit is determined to satisfy the following condition for given modulation index h [33],

$$\tau = \frac{T}{2h} = \frac{1}{2hB} \quad (2.24)$$

The phase difference between the signal and the delayed signal can be determined as

$$\begin{aligned}
\Delta\psi_{mark} &= \int_0^{\tau} (2\pi f_{IF} - 2\pi\Delta f) dt \\
&= 2\pi f_{IF}\tau - 2\pi\Delta f\tau \\
&= 2\pi f_{IF}\tau - 2\pi \frac{hB}{2} \frac{1}{2hB}
\end{aligned} \tag{2.25}$$

That is,

$$\Delta\psi_{mark} = 2\pi f_{IF}\tau - \frac{\pi}{2} \tag{2.26}$$

Similarly,

$$\Delta\psi_{space} = 2\pi f_{IF}\tau + \frac{\pi}{2} \tag{2.27}$$

Therefore, the phase difference between the signal and the delayed signal from the reference phase $2\pi f_{IF}\tau$ should be $-\frac{\pi}{2}$ for a mark signal and $\frac{\pi}{2}$ for a space signal. That means, a phase difference of π results between the mark and space signals.

2.4.5 Delay-demodulation with non-uniform LD FM response

In an actual system, the optical frequency is a time-variant function, even within a single bit duration, because of the non-uniform LD FM response. Thus the CPFSK modulated signal is distorted and the frequency shift is $2\delta f(t)$. Now the phase shift at the decision point is no longer $\pm\frac{\pi}{2}$.

As we know from equations (2.15) and (2.23), the demodulated output is

$$\begin{aligned}
v(t) &= u(t)u(t-\tau) \\
&= (A(t) \cos[2\pi f_{IF}t + \psi(t)]) (A(t-\tau) \cos[2\pi f_{IF}(t-\tau) + \psi(t-\tau)]) \\
&= \frac{1}{2} A(t)A(t-\tau) (\cos[2\pi f_{IF}(2t-\tau) + \psi(t) + \psi(t-\tau)] \\
&\quad + \cos[2\pi f_{IF}\tau + \psi(t) - \psi(t-\tau)])
\end{aligned} \tag{2.28}$$

The delay-demodulation is followed by a low pass filter which eliminates the high frequency signal. So the ultimate demodulated output is

$$v_o(t) = b(t) \cos[2\pi f_{IF}\tau + \psi(t) - \psi(t-\tau)] \tag{2.29}$$

The accumulated phase over the demodulation interval τ with respect to IF carrier phase ($2\pi f_{IF}\tau$),

$$\begin{aligned}\psi(t) - \psi(t - \tau) &= 2\pi \int_{t-\tau}^t \sum_{-\infty}^{\infty} a_n g(\lambda - nT) d\lambda \\ &+ \alpha_n(t) - \alpha_n(t - \tau) + \theta_n(t) - \theta_n(t - \tau)\end{aligned}\quad (2.30)$$

The total accumulated phase over the demodulation interval τ can be written as

$$\begin{aligned}\Delta\psi_T &= [2\pi f_{IF}\tau - 2\pi\Delta f\tau] \\ &+ \left[2\pi\Delta f\tau + 2\pi \int_{t-\tau}^t \sum_{-\infty}^{\infty} a_n g(\lambda - nT) d\lambda \right] \\ &+ [\alpha_n(t) - \alpha_n(t - \tau)] + [\theta_n(t) - \theta_n(t - \tau)]\end{aligned}\quad (2.31)$$

The IF centre frequency is adjusted such that

$$2\pi f_{IF}\tau = (m + \frac{1}{2})\pi, \quad m = 1, 2, \dots\quad (2.32)$$

Then,

$$\begin{aligned}\Delta\psi_T &= \left[(m + \frac{1}{2})\pi - \frac{\pi}{2} \right] + \left[2\pi\Delta f\tau + 2\pi \int_{t-\tau}^t \sum_{-\infty}^{\infty} a_n g(\lambda - nT) d\lambda \right] \\ &+ [\alpha_n(t) - \alpha_n(t - \tau)] + [\theta_n(t) - \theta_n(t - \tau)]\end{aligned}\quad (2.33)$$

In the above equation, the first two terms represent the correct phase difference in ideal case for desired frequency deviation when the transmitted bit is '1'. The next two terms represent the phase distortion due to the non-uniform FM response of the laser including the pattern dependent effect. The next two terms represent the phase distortion due to laser phase noise. The last two terms represent the phase distortion due to receiver noise including the shot noise and thermal noise.

For IF filter bandwidth of $2B$ and typical values of h used in CPFSK system ($h \leq 1$), the correlation between the phase noise samples due to receiver thermal and shot noise, separated by the delay time $\tau (= \frac{T}{2h})$ is negligibly small for $\tau > 0.5T$ [47]. This leads to the assumption that $\theta_n(t)$ and $\theta_n(t - \tau)$ are uncorrelated and, therefore, independent. The quantum phase noise samples $\alpha_n(t)$ and $\alpha_n(t - \tau)$ are also considered to be independent.

2.4.6 Data decision

Data decision can be made using the polarity of the output signal $v_o(t)$. The polarity depends on the phase of the signal $v_o(t)$. When '1' is transmitted, the correct phase would be $(m + \frac{1}{2})\pi - \frac{\pi}{2}$, $m = 1, 2, 3, \dots$. So an error will occur if $-\pi < \Delta\psi_{mod\ 2\pi} < 0$. Similarly, an error will occur when '0' is transmitted if $0 < \Delta\psi_{mod\ 2\pi} < \pi$. That means, error will occur when $0 < |\Delta\psi_{mod\ 2\pi}| < \pi$.

Rewriting the equation (2.33), the total accumulated phase,

$$\begin{aligned} \Delta\psi_T &= [(m + \frac{1}{2})\pi - \frac{\pi}{2}] + [2\pi\Delta f\tau \\ &+ 2\pi a_0 \int_0^\tau g(\lambda)d\lambda + 2\pi \int_{t-\tau}^t \sum_{-\infty}^{\infty} a_n g(\lambda - nT)d\lambda \\ &+ [\alpha_n(t) - \alpha_n(t - \tau)] + [\theta_n(t) - \theta_n(t - \tau)] \end{aligned} \quad (2.34)$$

where \sum' excludes $n = 0$. It is to be noted the desired phase change over the demodulation period is disturbed by the laser phase noise, shot noise and thermal noise of the receiver and the pattern dependent effect due to non-uniform FM response characteristics. From the above equation we get the phase error from the desired phase due to non-uniform LD FM response as

$$\begin{aligned} \theta(t) &= 2\pi\Delta f\tau - 2\pi \int_0^\tau g(\lambda)d\lambda + 2\pi \int_{t-\tau}^t \sum_{-\infty}^{\infty} a_n g(\lambda - nT)d\lambda \\ &= \frac{\pi}{2} - 2\pi \int_0^\tau g(\lambda)d\lambda + 2\pi \int_{t-\tau}^t \sum_{-\infty}^{\infty} a_n g(\lambda - nT)d\lambda \end{aligned} \quad (2.35)$$

where a_0 is chosen to be -1 because the IF frequency is $f_{IF} - \Delta f$ when '1' is transmitted in ideal case. The average phase error from the desired phase is, therefore,

$$\theta_0 = \frac{\pi}{2} - 2\pi \int_0^\tau g(\lambda)d\lambda \quad (2.36)$$

The term $2\pi \int_{t-\tau}^t \sum a_n g(\lambda - nT)d\lambda$ in equation (2.35) represents the pattern dependent modulation effect due to non-uniform LD FM response.

The phase error due to non-uniform LD FM response can be rewritten as

$$\theta(t) = \theta_0 + \theta_{iis}(t) \quad (2.37)$$

where

$$\theta_{isi}(t) = 2\pi \int_{t-\tau}^t \sum_{-\infty}^{\infty} a_n g(\lambda - nT) d\lambda \quad (2.38)$$

The equation (2.37) reveals that the non-uniform LD FM response produces an average phase error θ_o due to distortion of the signal bit pulse shape and a random phase error $\theta_{isi}(t)$ which represents the effective random phase error due to pattern randomness effect.

The statistics (pdf, $p(\theta)$) of the random phase error $\theta(t)$ can be determined from the knowledge of the moments of the random process $\theta_{isi}(t)$. The characteristic function of $\theta_{isi}(t)$ can be shown to be given by [34]

$$\begin{aligned} F(j\psi) &= \sum_{r=1}^{\infty} \frac{(j\psi)^{2r}}{(2r)!} M_{2r} \\ &= \prod_{r=1}^{\infty} \cos[\psi g_r(t')] \end{aligned} \quad (2.39)$$

where M_{2r} represents the $2r$ th moments of $\theta_{isi}(t)$, $g_r(t') = |g_o(t' - rT)|$ with $g_o(t) = 2\pi \int_{t-\tau}^t g(t) dt$. The odd order moments are all found to be zero and the even order moments can be evaluated using the following recursive relation [34]

$$M_{2r} = Y_{2r}(N) \quad (2.40)$$

$$Y_{2r}(i) = \sum_{j=0}^r \binom{2r}{2j} Y_{2j}(i-1) g_r^{(2r-2j)} \quad (2.41)$$

where N is the number of terms in the summation in (2.38) and the brackets represents binomial coefficients. The pdf of $\theta(t)$ can be obtained by taking the inverse Fourier transform of $F(j\psi)$.

2.4.7 Bit Error Rate

The phases $\alpha_n(t)$ and $\alpha_n(t - \tau)$ are assumed to be independent, so also are the phases $\theta_n(t)$ and $\theta_n(t - \tau)$. Further, the phase noise due to shot and receiver noise is statistically independent of that due to the quantum phase noise. We can, therefore,

invoke the modified Blachman's equation to write the error probability expression [8], [16]. For the symmetrical system $p(1/0) = p(0/1) = BER$. So the error probability conditioned on a given realization of the phase error $\theta(t)$, is [47]

$$P_e|\theta = \frac{1}{2} - \frac{1}{2}\rho \exp(-\rho) \sum_0^{\infty} \frac{(-1)^n}{2n+1} \left[I_n\left(\frac{\rho}{2}\right) + I_{n+1}\left(\frac{\rho}{2}\right) \right]^2 \times \exp[-(2n+1)^2\pi\Delta\nu\tau] \cos[(2n+1)\theta] \quad (2.42)$$

where,

$\rho = \text{IF SNR for bit '1'}$,

$\Delta\nu = \text{sum of the transmitting and local oscillator LD linewidths}$, and $I_n(x) = \text{modified Bessel function of the first kind of } n\text{th order}$.

The unconditional bit error probability of the CPFASK system is, therefore, obtained by averaging $P_e|\theta$ with respect to the pdf of θ i.e. $p(\theta)$, as

$$P_e = E_{\theta}[P_e|\theta] = \int_{-\infty}^{\infty} (P_e|\theta)p(\theta)d\theta \quad (2.43)$$

In case of ideal FM response of laser, $m(t) = -\Delta f\delta(t)$ when bit '1' is transmitted. So the mean value of θ , $\theta_0 = 2\pi\Delta f\tau - 2\pi a_0\Delta f\tau = 0$ [$a_0 = -1$ for bit '1']]. Similarly, $2\pi \int_0^T \sum a_n p(t - nT) dt = 0$, because there is no pattern dependent effect. So the bit error rate for ideal LD FM response will be simply,

$$P_e = \frac{1}{2} - \frac{1}{2}\rho \exp(-\rho) \sum_0^{\infty} \frac{(-1)^n}{2n+1} \left[I_n\left(\frac{\rho}{2}\right) + I_{n+1}\left(\frac{\rho}{2}\right) \right]^2 \times \exp[-(2n+1)^2\pi\Delta\nu\tau] \quad (2.44)$$

But in case of non-uniform FM response of laser, the equations (2.42) and (2.43) are to be employed. Since θ is mod 2π , the equation (2.38) is to be written as

$$P_e = \sum_{-\infty}^{\infty} \int_{-\pi}^{\pi} (P_e|\theta)p(\theta - 2n\pi)d\theta \quad (2.45)$$

This is the bit error rate expression for a coherent optical heterodyne CPFASK delay-demodulation system.

2.5 Optical CPFSK with Linecoding

It is observed that appropriate linecoding of laser driving signal can overcome the adverse effect of non-uniform FM response of the transmitting laser. Alternate-Mark-Inversion (AMI) linecoding is employed in this work.

2.5.1 AMI Encoding

This is a ternary linecoding. The modulator has $q = 2$ states, say, Σ_+ and Σ_- , and the source is binary. The modulator responds to a source symbol '0' with a zero waveform and to a source symbol '1' with waveform $s(t)$ or $-s(t)$, according to whether its state is Σ_+ or Σ_- respectively. Source symbols '1' make the modulator change its state. The tabular and state diagram representation of this signal are shown in figure 2.4. This code is also known as bipolar code.

It is intuitive that this encoding method has the advantage of reducing the dc component of the signal because a pulse of one polarity is always followed by a pulse of opposite polarity.

2.5.2 BER with AMI Linecoding

The linecoder shown in figure 2.5 can be viewed as a linear time-invariant filter which acts on the input data signal $I(t)$ to generate an output sequence of data given by [3]

$$I'(t) = \sum_{n=-\infty}^{\infty} b_n q'(t - nT). \quad (2.46)$$

Here $q'(t)$ has the Fourier transform as follows

$$Q'(f) = G'(f)P(f) \quad (2.47)$$

where

$$G'(f) = \sum_{n=0}^{k-1} g'_n e^{-2\pi n f T} \quad (2.48)$$

| | | |
|--------------------------------|------------|------------|
| $\alpha_n \backslash \sigma_n$ | Σ_+ | Σ_- |
| 0 | 0 | 0 |
| 1 | $s(t)$ | $-s(t)$ |

| | | |
|--------------------------------|------------|------------|
| $\alpha_n \backslash \sigma_n$ | Σ_+ | Σ_- |
| 0 | Σ_+ | Σ_- |
| 1 | Σ_- | Σ_+ |

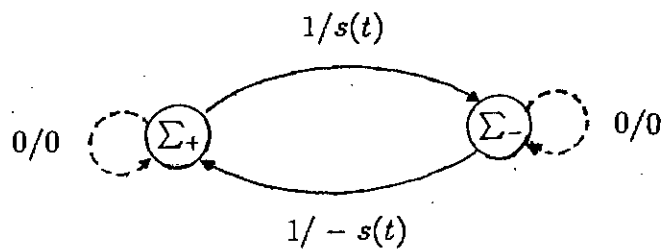


Figure 2.4: Tabular and state diagram of Alternate-Mark-Inversion (AMI) linecoding.

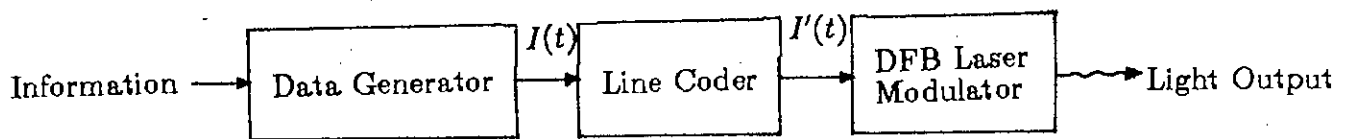


Figure 2.5: Block diagram of an optical transmitter with linecoder.

is the transfer function of the linecoder, and the sequence of symbols $\{b_n\}$ is generated to avoid error propagation by a precoder defined by

$$a_n = \sum_{i=0}^{k-1} g'_i b_{n-i}, \quad \text{mod } 2 \quad (2.49)$$

The k coefficients $g'_0, g'_1, g'_2, \dots, g'_{k-1}$ are usually integers and can be properly chosen to generate the AMI linecoding scheme.

From equation (2.45) it is also clear that if the symbols of the sequence $\{a_n\}$ are independent and identically distributed (iid), so also are the symbols of the sequence $\{b_n\}$. In the case of CPFSK with NRZ data we have seen that a_n are iid, and each elementary pulse $p(t)$ is filtered by $m(t)$. In the case of CPFSK with linecoded data we simply have $\{b_n\}$, which are again iid, but now the elementary pulse shape $p(t)$ of the individual data bit is filtered by an equivalent impulse response, $g'(t) * m(t)$, where $g'(t) = F^{-1}[G'(f)]$ is the pulse shaping function due to linecoding. For AMI linecoded signal, the pulse shaping function is obtained from the following $G'(f)$ [3],

$$G'(f) = 1 - e^{-j2\pi fT} \quad (2.50)$$

Because of the precoding employed, it is always possible to adopt symbol-by-symbol decisioning.

It is therefore possible to apply the same procedure for the BER evaluation of CPFSK with NRZ data in section 2.4.7 to the present situation with linecoded data by merely replacing $g(t)$ in the previous case by

$$\begin{aligned} g''(t) &= p(t) * m(t) * h(t) * g'(t) \\ &= g(t) * g'(t) \end{aligned} \quad (2.51)$$

2.6 Results and Discussion

In this section we present the performance results of optical heterodyne CPFSK receiver with delay-demodulation considering the effect of laser phase noise, receiver

noise and non-uniform FM response of lasers. The bit error rate of delay-demodulation CPFSK receiver is computed following the theoretical analysis given in section 2.4 and 2.5. Computations are carried out at a bit rate of 2.5 Gb/s for both NRZ and AMI encoded data pattern. The non-uniform FM response $M(f)$ of a practical DFB laser shown in figure 2.1 is used for numerical computations. The FM impulse response $m(t)$ obtained by inverse Fourier transform of $M(f)$ is shown in figure 2.2. For a laser with ideal FM response $M(f)$ is flat and $m(t)$ is a dirac delta function. Figure 2.2 indicates that in case of non-uniform FM response $m(t)$ has a finite duration which introduces interference pattern for long input bit sequence. We define the modulation index $h = 2\Delta fT$, where Δf is the peak frequency deviation. For a given modulation index h , normalization of $M(f)$ is done such that the peak frequency deviation over a bit period equals Δf .

The effective pulse shape $p'(t) = p(t) * m(t)$ for NRZ data is shown in figure 2.6. From the figure it is noticed that though $p(t)$ is rectangular, the effective pulse shape gets distorted due to the presence of non-uniformity in the FM response $M(f)$ and continues for a large number of bit duration. When AMI linecoding is employed, the resultant effective pulse shape $p''(t) = p(t) * m(t) * g'(t)$ is shown in figure 2.7. Comparison of this curve with figure 2.6 reveals that there is an improvement in the effective pulse shape due to AMI encoding and it goes to zero after a few input bits and thus reduces the distortion introduced by the non-uniform FM response.

The plots of average phase error θ_o at the output of the delay-demodulator are shown in figure 2.8 and 2.9 for NRZ and AMI encoded data pattern respectively. For NRZ data the average phase error increases with increasing modulation index h and crosses the zero value at $h = 1.15$. On the otherhand, for AMI encoded data, the phase error decreases and attains a minimum value corresponding to an optimum value of $h = 0.9$ after which it again increases with increasing h .

The probability density function (pdf) of the random phase error $\theta(t)$ at the demod-

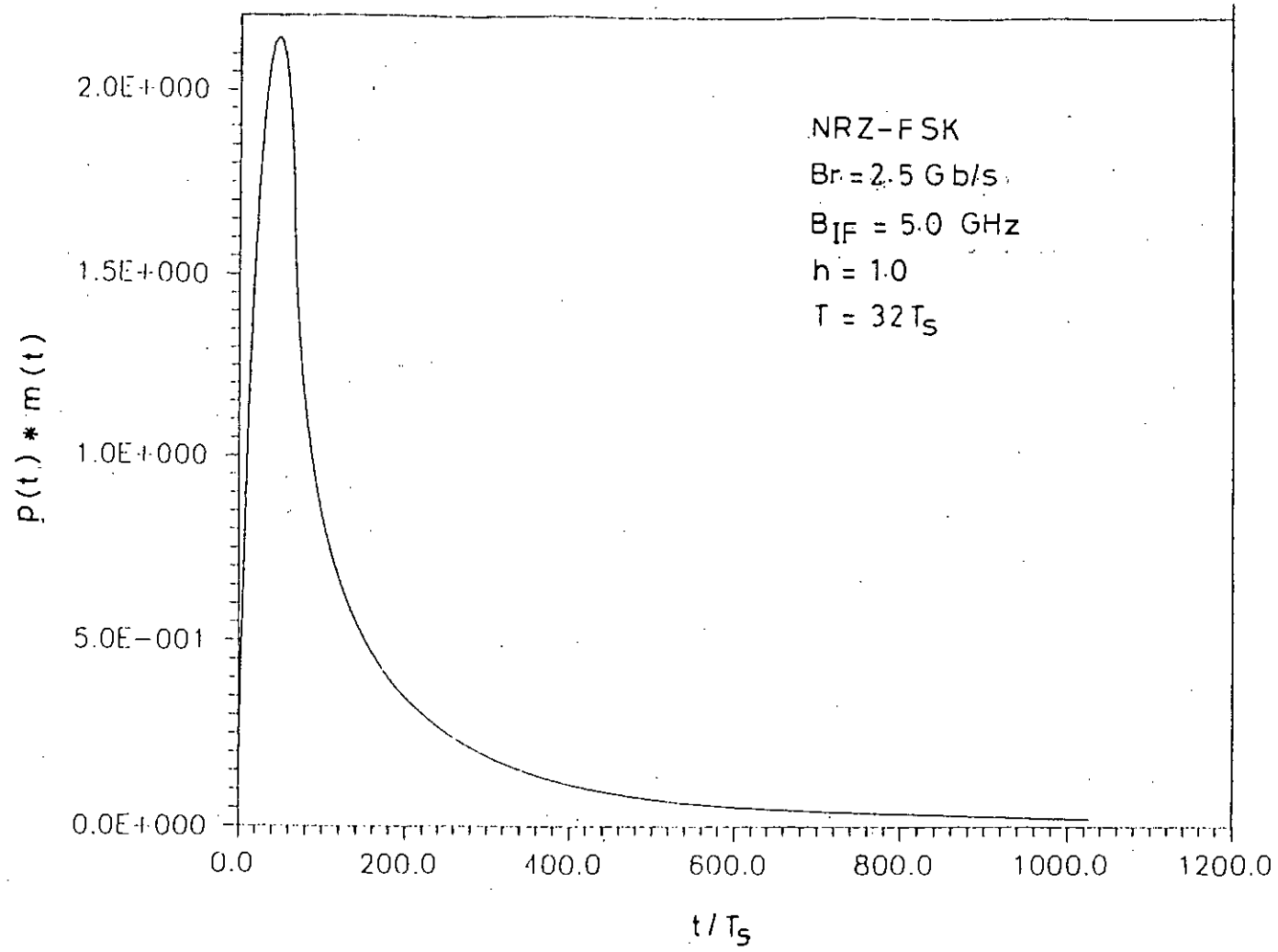


Figure 2.6: Effective pulse shape for NRZ data.

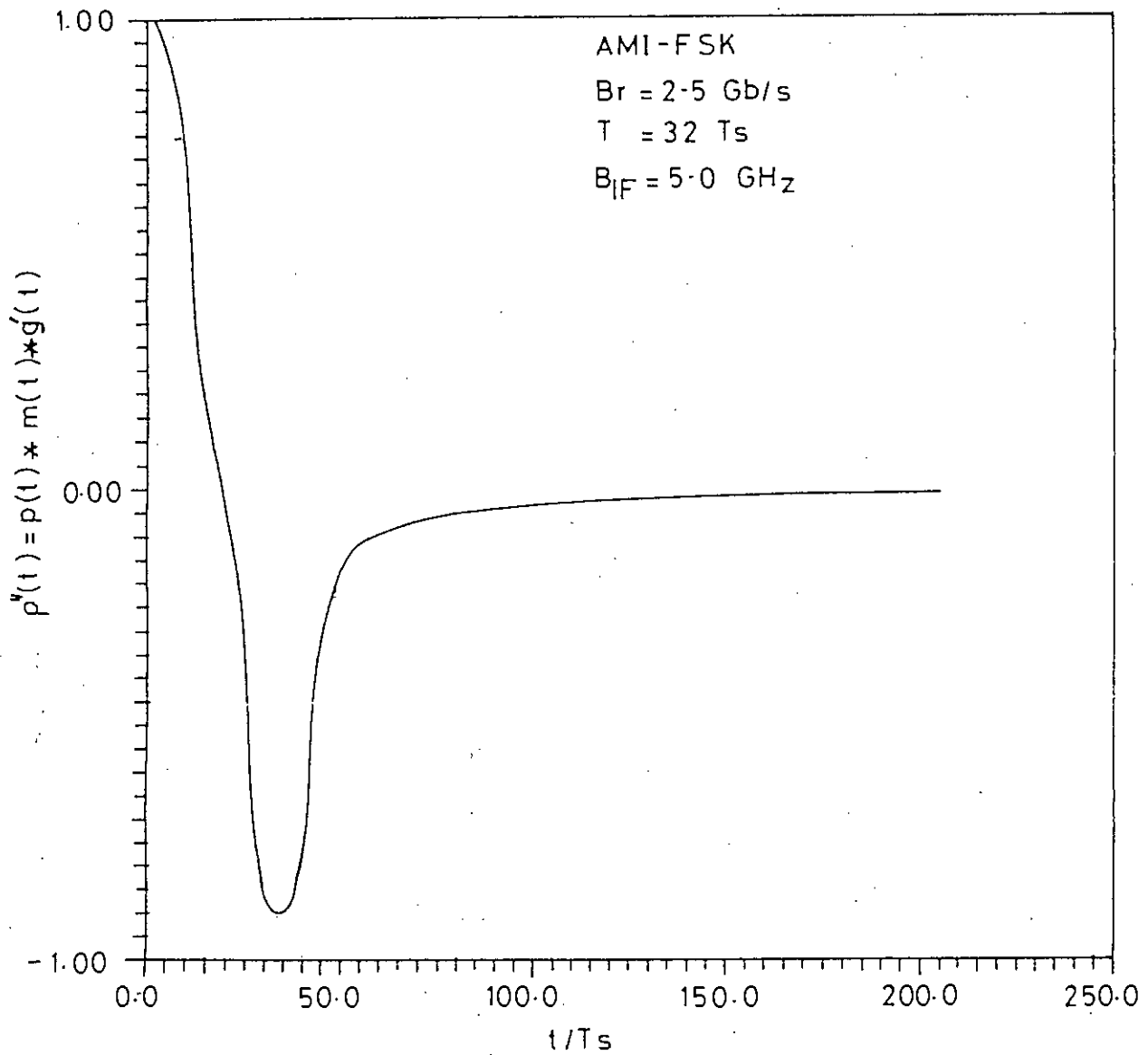


Figure 2.7: Effective pulse shape for AMI encoded data.

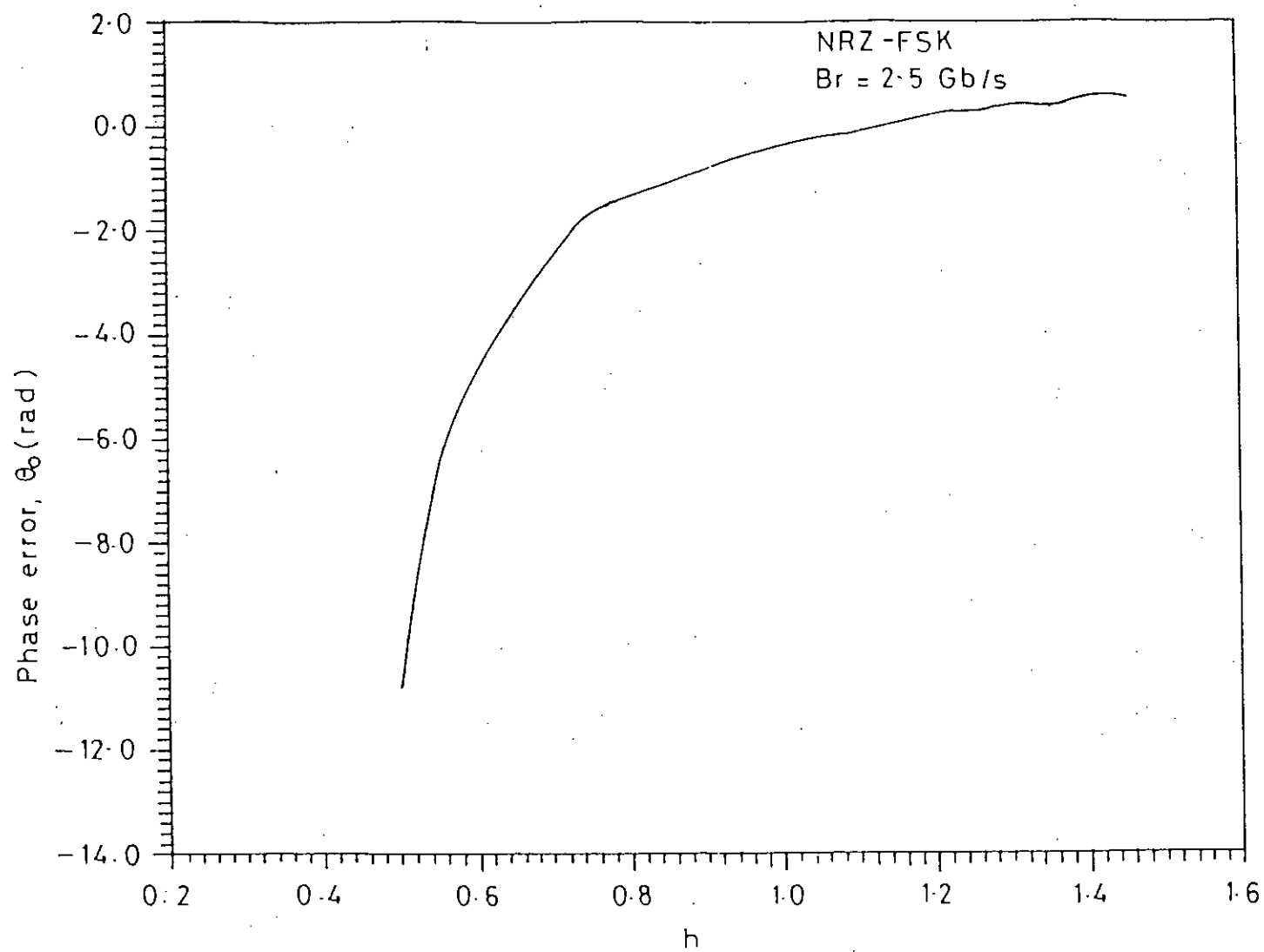


Figure 2.8: The average phase error vs. modulation index for NRZ data.

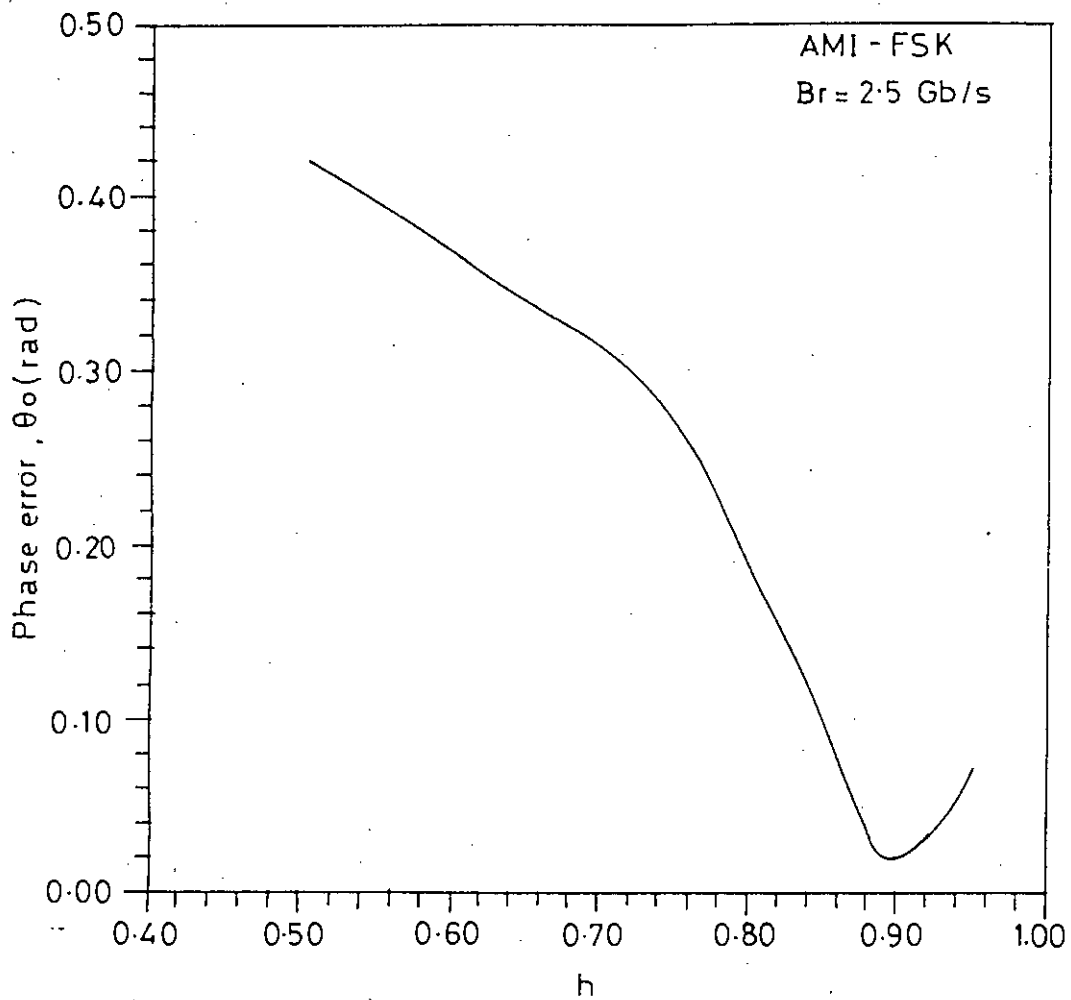


Figure 2.9: The average phase error vs. modulation index for AMI coded data.

ulator output is plotted with $h = 0.83$ in figure 2.10 and with $h = 1.15$ in figure 2.11 for normalized laser linewidth $\Delta\nu T = 0.0$. For an 'ideal FM' laser, $p(\theta)$ is an impulse at $\theta = 0.0$. In the present case, the values of $p(\theta)$ tends to be zero at multiples of π . At other values of θ greater than $\frac{\pi}{2}$, the probability of occurrence holds its value at almost a constant value and does not decrease towards zero with increasing θ . The value of $p(\theta)$ at which it remains almost constant is about 10^{-7} for $h = 0.83$ and 10^{-8} for $h = 1.15$. This tendency of the pdf $p(\theta)$ will result in bit error rate floor in the receiver performance which can be lowered by lowering the modulation index h .

Using the pdf $p(\theta)$, the probability of bit error for CPFSK receiver is then computed at a bit rate of 2.5 Gb/s for NRZ and AMI encoded data without including the effect of laser phase noise ($\Delta\nu T = 0.0$) as shown in figure 2.12 for several values of modulation index h . To meet the optimum demodulation condition, the IF bandwidth B_{IF} is kept at twice the bit rate i.e. 5 Gb/s. The figure depicts that CPFSK system suffers bit error rate floor for NRZ data pattern at around 10^{-4} and 10^{-5} for $h = 1.0$ and $h = 1.15$ respectively. The error rate floor can be lowered by increasing the value of modulation index upto a certain limit after which floor again goes upward. There is a minimum error rate floor that occurs at 10^{-5} corresponding to optimum value of $h = 1.15$. Further increase in h causes the floor to go upward. A sensitivity of $\text{BER}=10^{-9}$ can never be achieved by increasing signal power. When AMI encoding is employed, the error rate floor is significantly lowered to 10^{-9} and the system suffers only a power penalty of approximately 3.0 dB at $\text{BER}=10^{-9}$ compared to the 'ideal FM' case.

In the presence of laser phase noise, the BER performance is depicted in figure 2.13 for both NRZ and AMI encoded data for $h = 1.0, 1.15$ with $\Delta\nu T = 10^{-3}$. Comparison with figure 2.12 reveals that the error rate floor is slightly increased for NRZ-FSK and for AMI-FSK. The penalty at $\text{BER}=10^{-9}$ is also increased by 1.6 dB. This additional penalty is due only to laser phase noise.

Figure 2.14 shows that the plots of BER vs. SNR for NRZ-FSK and AMI-FSK for

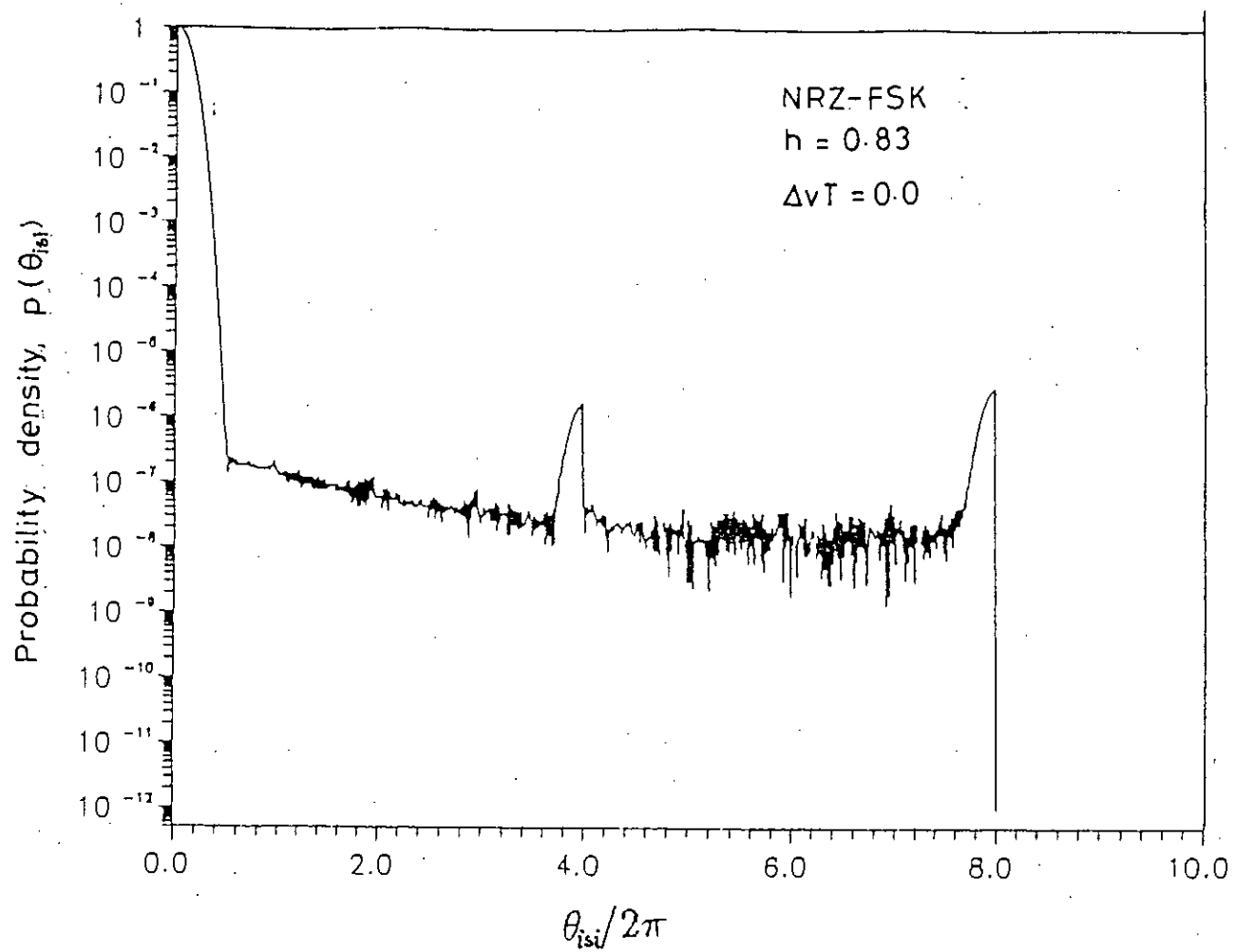


Figure 2.10: Probability density function of phase error vs. θ for $h=0.83$.

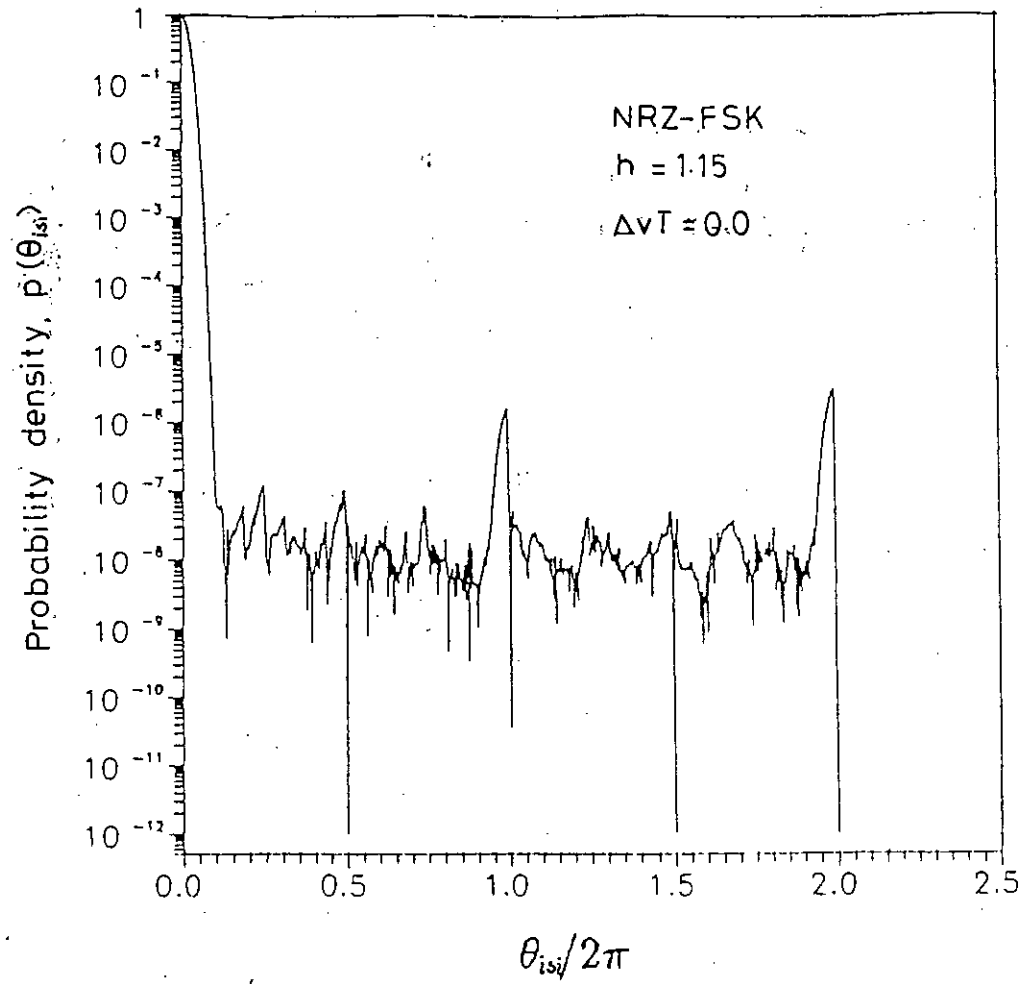


Figure 2.11: Probability density function of phase error vs. θ for $h=1.15$.

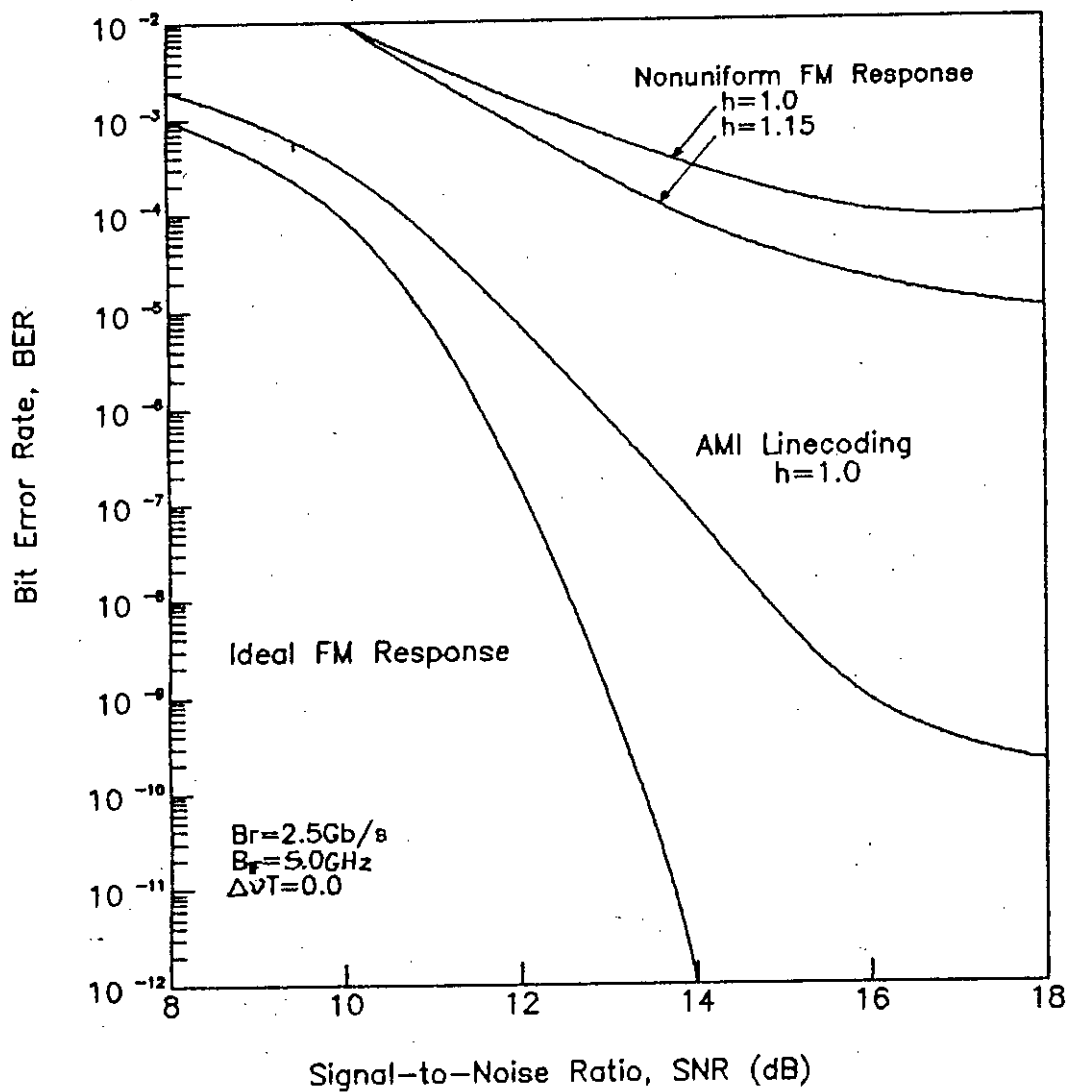


Figure 2.12: Bit error rate performance of optical CPFSK system with delay-demodulation for NRZ and AMI coded data with $\Delta\nu T = 0.0$.

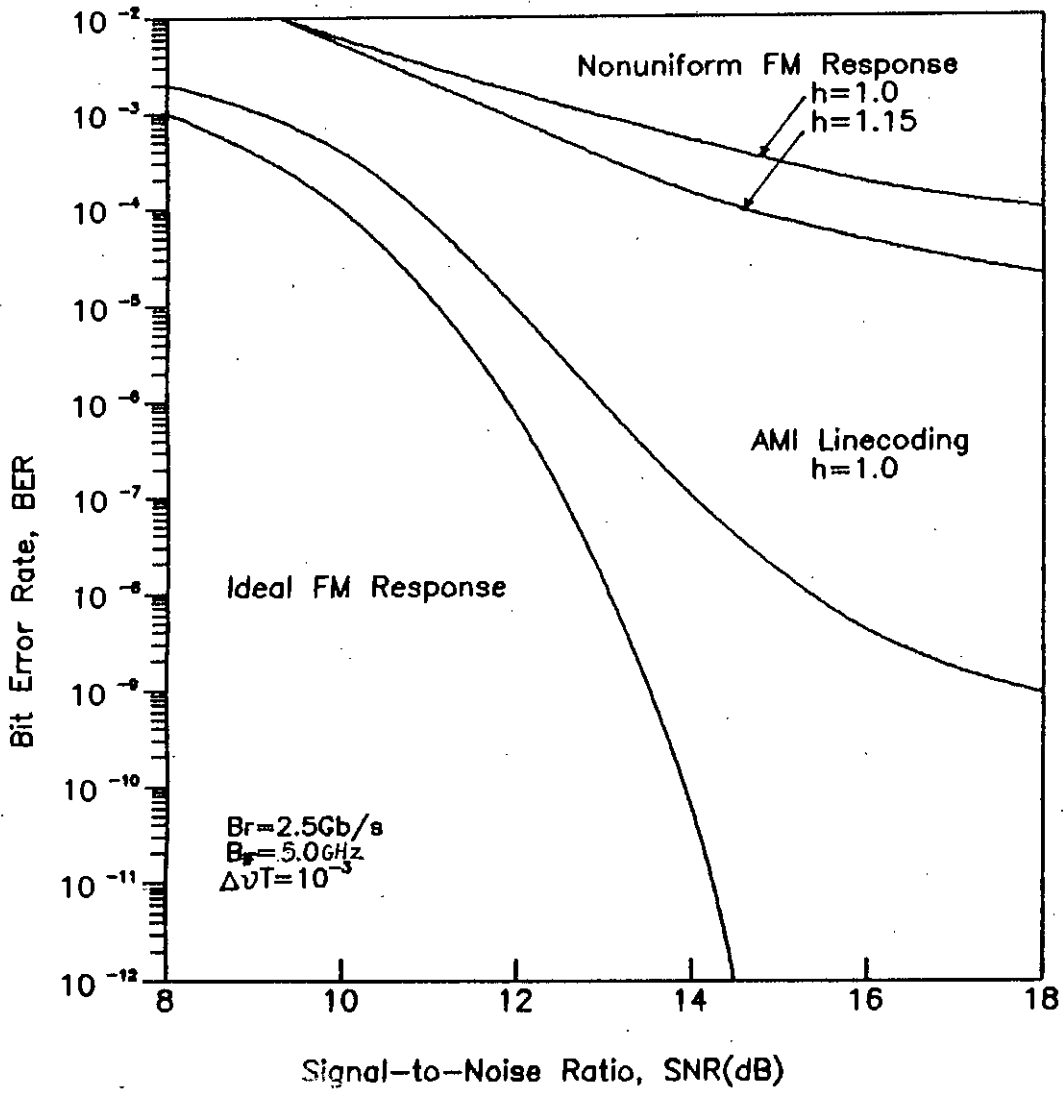


Figure 2.13: Bit error rate performance of optical CPFSK system with delay-demodulation for NRZ and AMI data with $\Delta\nu T = 10^{-3}$

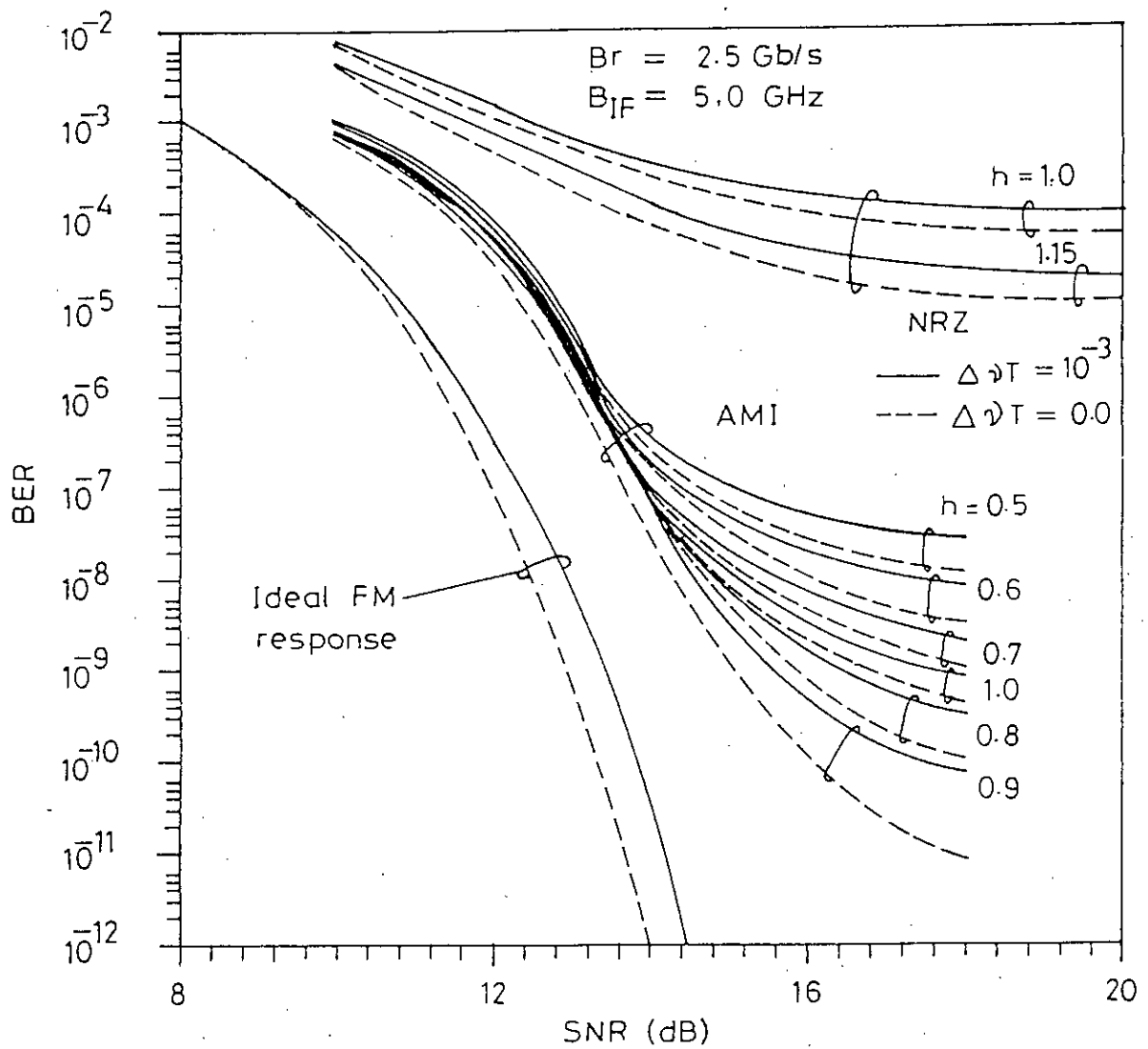


Figure 2.14: Bit error rate performance of optical CPFSK system with delay-demodulation for NRZ and AMI coded data with $\Delta\nu T = 0.0$ & 10^{-3} .

several values of modulation index h with $\Delta\nu T = 0.0, 10^{-3}$ and IF bandwidth $B_{IF}=5.0$ GHz. It is noticed that the error rate floor occurs at different values of BER depending on the value of modulation index h . When $h = 0.5$, the BER floor occurs at around 5×10^{-8} . As h is increased the floor goes downward until it reaches its minimum value at around 10^{-10} for $h = 0.9$. Further increase in the values of h causes the BER floor to occur at higher values of BER. Thus the system exhibits a minimum BER floor corresponding to an optimum value of $h = h_{opt}$ which is equal to 0.9 for $\Delta\nu T = 10^{-3}$. The optimum value of h corresponds to an optimum value of demodulation time $\tau = \tau_{opt}$.

Further, compared to 'ideal FM' case with $\Delta\nu T = 0.0$, there is a penalty in signal power to achieve $BER=10^{-9}$ which gradually decreases as h is increased from 0.5 and it reaches its minimum value of 2.2 dB for $\Delta\nu T = 10^{-3}$ at the optimum value of $h = 0.9$. Further increase in h causes the penalty to be increased further.

The plots of BER vs. SNR with $\Delta\nu T$ as a parameter is shown in figure 2.15 for two different values of $h = 0.8, 0.9$. It is noticed that at a given value of modulation index, the BER floor and hence the power penalty increases with increasing phase noise. At $\Delta\nu T = 10^{-4}$ with $h = 0.9$ the BER floor occurs below 10^{-12} and it occurs at around 10^{-9} when $\Delta\nu T$ is increased to 0.01. Further increase in phase noise causes the BER floor to occur above 10^{-9} and the desired sensitivity can never be achieved. The performance degradation due to phase noise is attributed to the fact that as linewidth increases the frequency spectrum of the transmitting laser widens resulting in more frequency noise in the laser output.

The power penalty suffered by the system to achieve $BER=10^{-9}$ due to the combined effect laser phase noise and non-uniform FM response is then determined for the plots of BER vs. SNR as in figure 2.12 through 2.15 for several values of h and $\Delta\nu T$. The plots of penalty vs. normalized linewidth $\Delta\nu T$ is given in figure 2.16 for various modulation index. It is found that the penalty increases with increasing value of $\Delta\nu T$. For example, when $h = 0.7$, the penalty is 4.4 dB for $\Delta\nu T = 10^{-4}$ and it is 5.7 dB

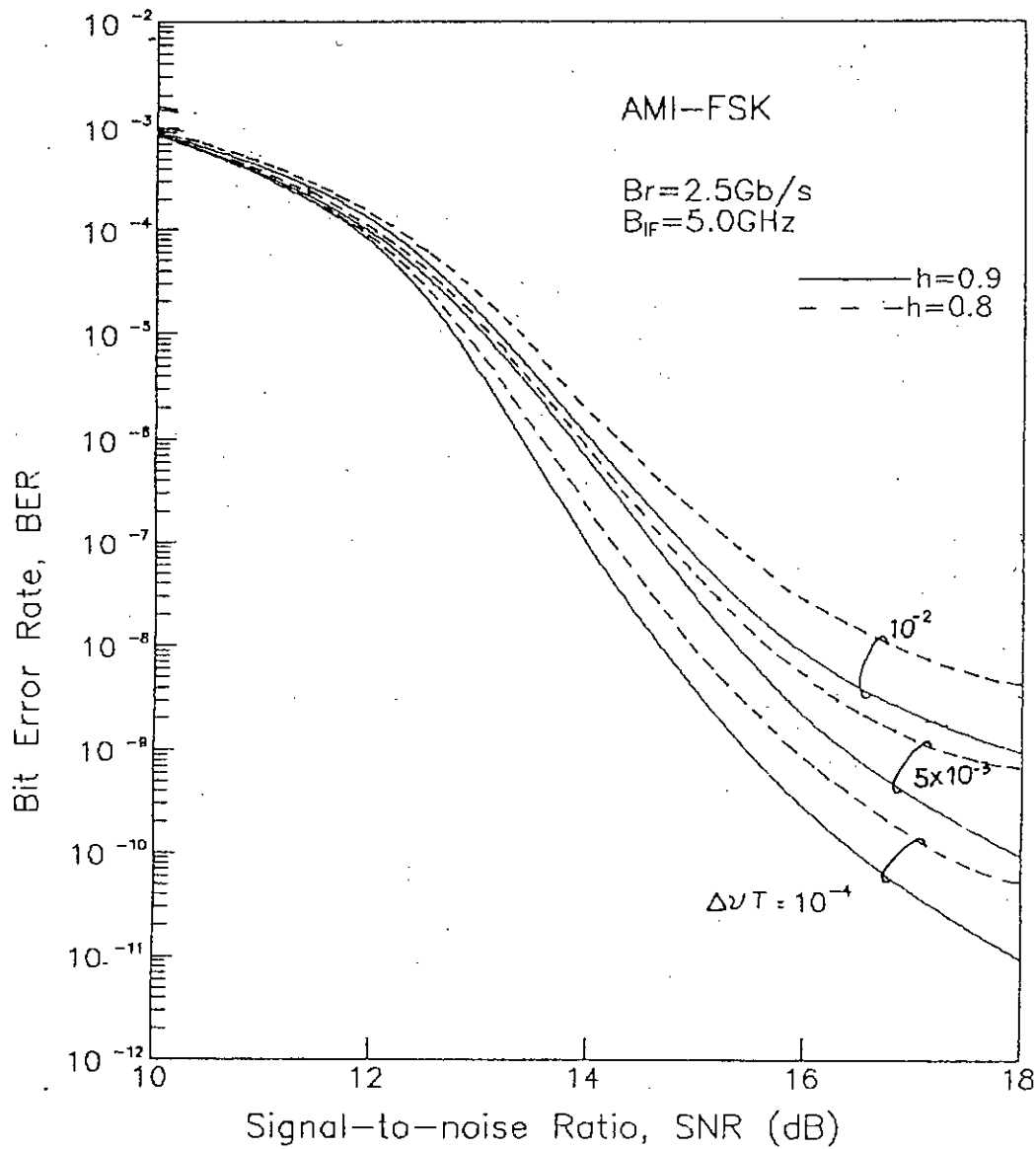


Figure 2.15: Bit error rate performance of optical CPFSK system with delay-demodulation with AMI coded data for several values of modulation index and normalized linewidth

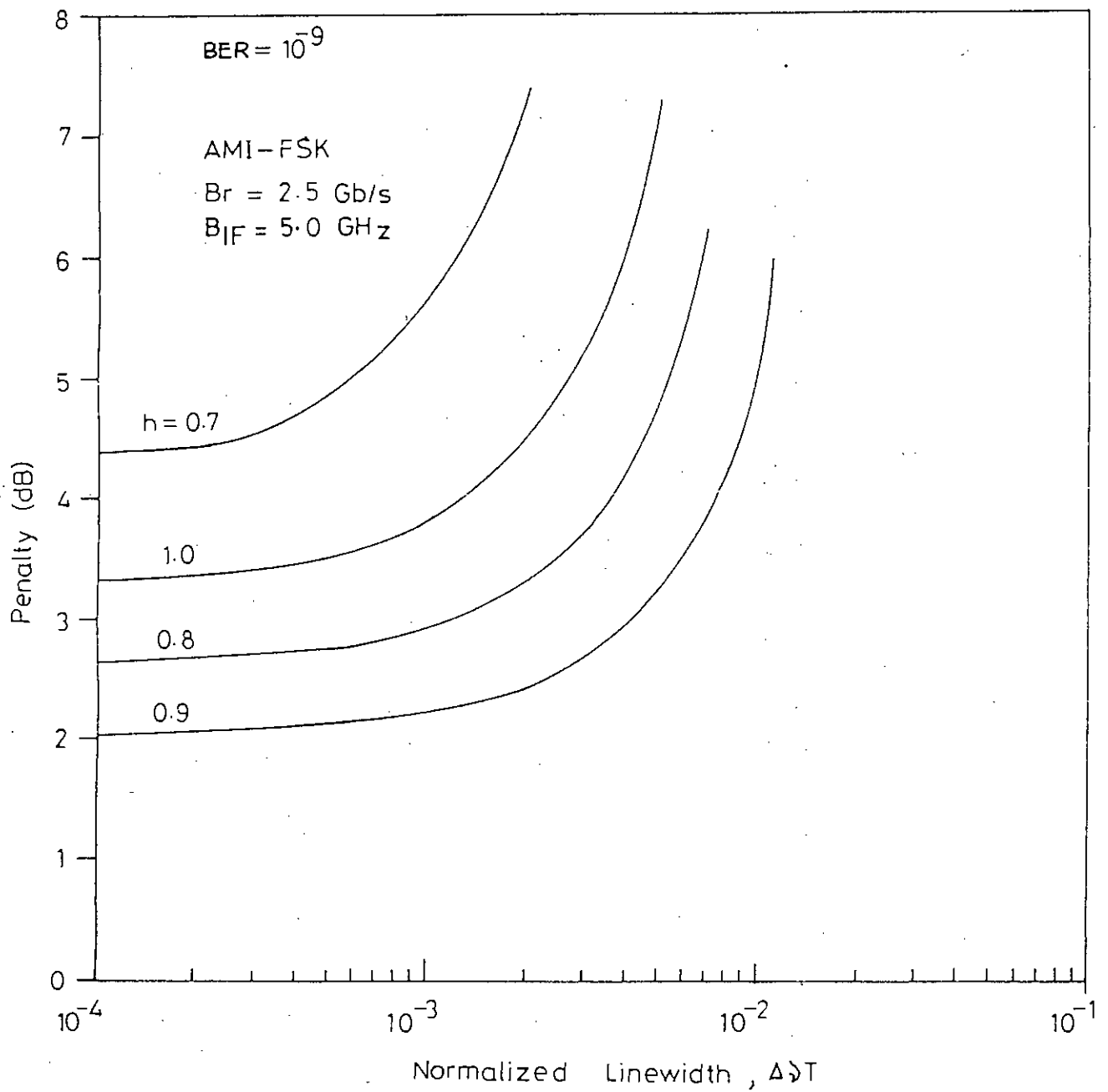


Figure 2.16: Power penalty vs. normalized linewidth for several values of modulation index with AMI encoded data.

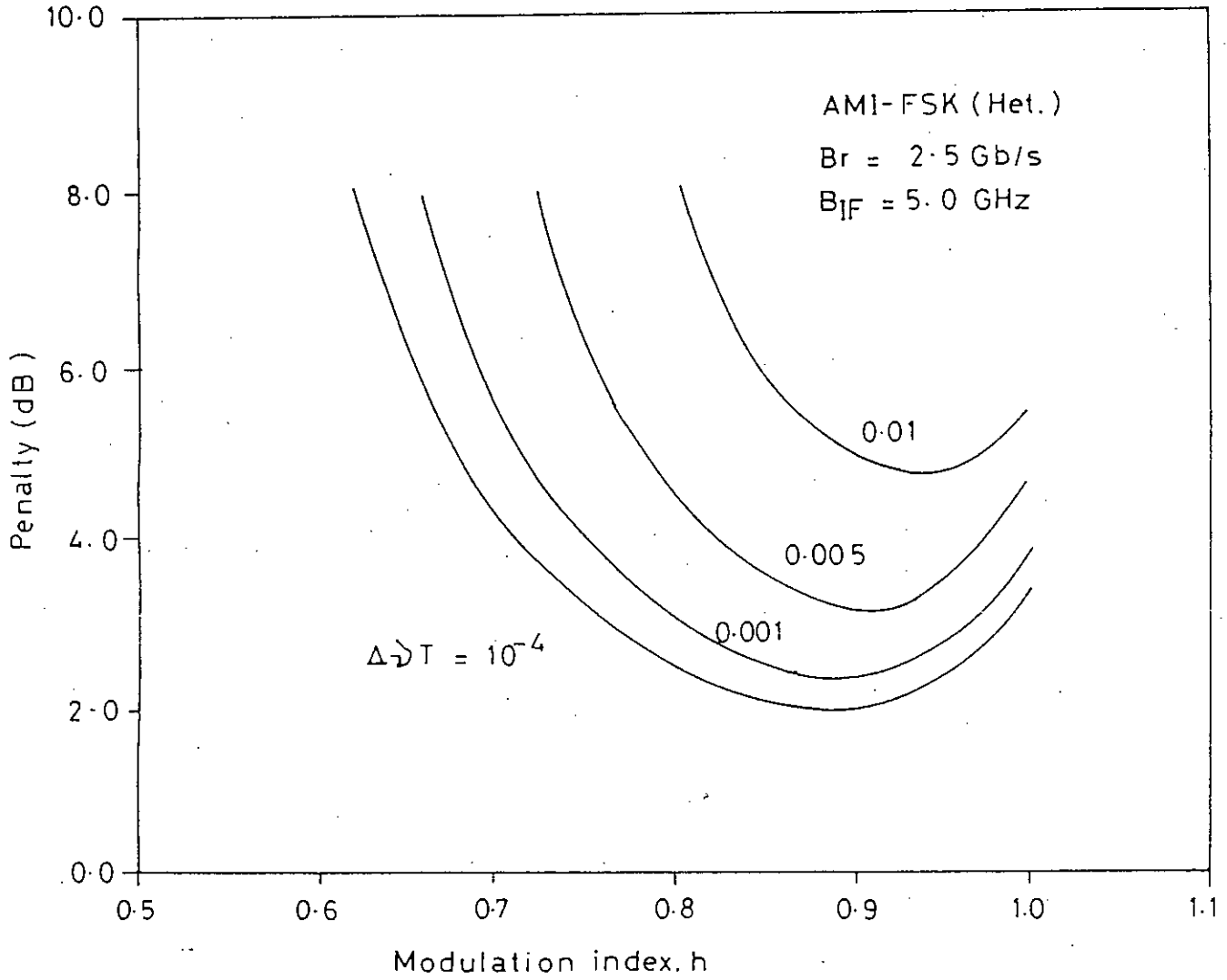


Figure 2.17: Power penalty vs. modulation index for several values of normalized linewidth.

when $\Delta\nu T = 10^{-3}$. However, for a particular value of $\Delta\nu T$, the penalty can be greatly reduced by increasing the value of modulation index. For example, for $\Delta\nu T = 10^{-4}$, the penalty can be reduced for 4.4 dB to 2.05 dB by increasing the modulation index from 0.7 to 0.9. The amount of reduction is more pronounced at larger values of linewidth. This is due to the fact that at lower values of linewidth, the thermal noise and shot noise at the photodetector output are much more dominant compared to excess noise due to laser phase noise. Therefore, at smaller values of linewidth larger values of h does not have significant contribution towards noise reduction.

Figure 2.17 shows the variation of power penalty with modulation index for different values of linewidth. It is again noticed that the penalty decreases with increasing h and attains a minimum value corresponding to a optimum value of h at a given value of $\Delta\nu T$. Further increase in h causes the penalty to be increased further. If a modulation index greater than the optimum value is chosen, the system suffers a penalty which is larger than that resulted by choosing a value smaller than the optimum value. It is due to the fact that for modulation index less than optimum value, the excess noise due to phase noise dominates over the shot and thermal noise. As h is increased, the separation between 'mark' and 'space' frequencies increases which reduces the intersymbol interference due to phase noise and the penalty reduces to a minimum value corresponding to an optimum value of h . Further increase of h above the optimum value causes the spectrum to be widened further which in turn reduces the signal power within the IF filter bandwidth. As a result the bit error rate and hence the penalty increases.

Further the optimum value of h and hence the optimum demodulation time is different for different values of linewidth. The optimum h is slightly higher for higher values of linewidth. As for example, the optimum value of h is 0.9 for $\Delta\nu T = 10^{-4}$ whereas it is 0.94 when $\Delta\nu T$ is increased to 0.01.

Finally, the comparison of the theoretical results with theoretical and experimental results reported earlier [33] is provided in figure 2.18. The parameters chosen for numer-

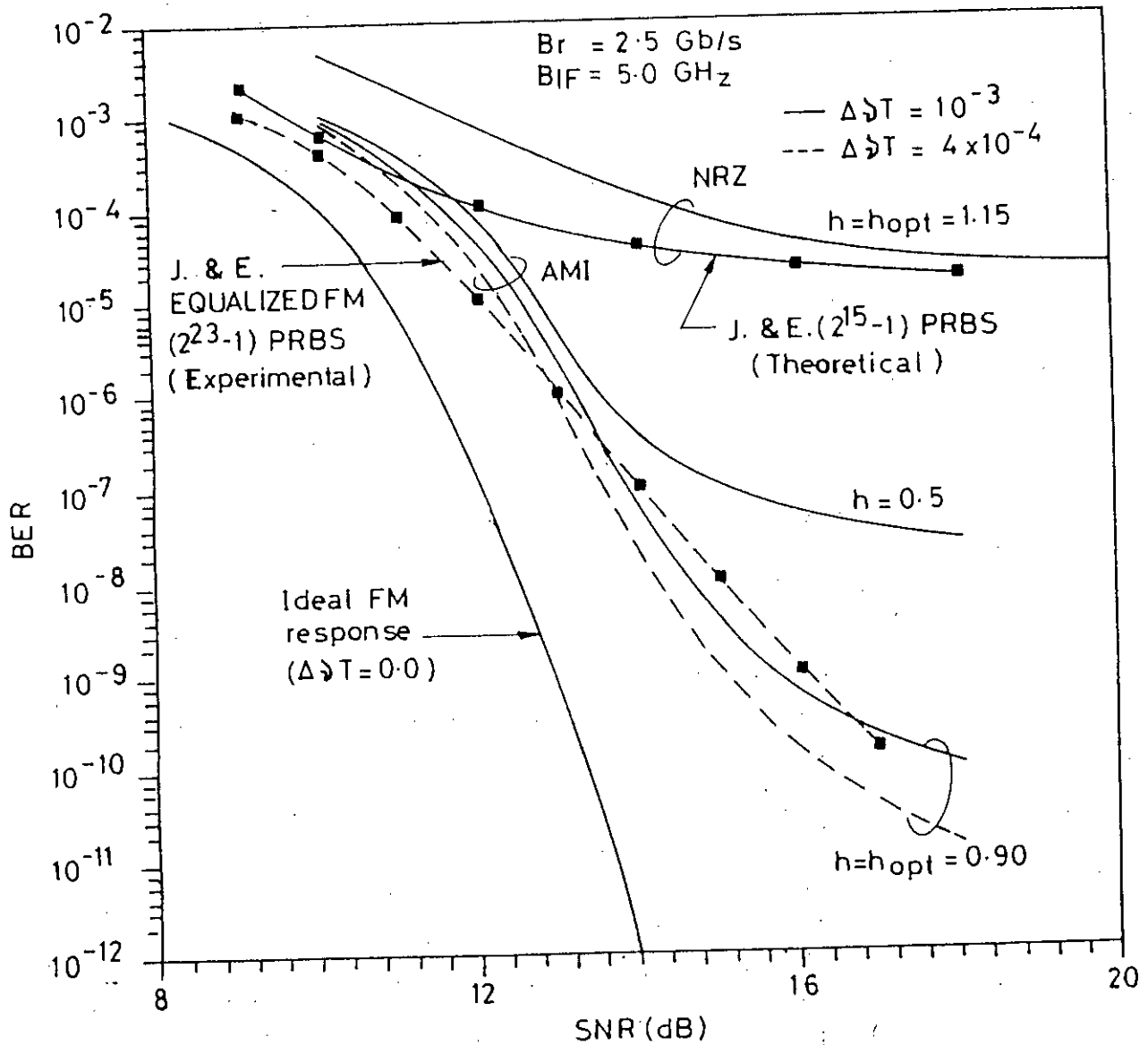


Figure 2.18: Comparison of theoretical BER results with that of published paper [33].

ical computations are same as in experimental demonstration in Ref. 33. It is evident that the BER floor suffered by NRZ-FSK system occurs at around 5×10^{-5} which is very close to that reported theoretically by Jacobsen and Emura [33].

The figure also compares the theoretical results of AMI-coded FSK system with experimental results with equalized FM response and NRZ data reported in Ref. 33. The experimental curve corresponds to an optimum modulation index $h = 0.83$ and $\Delta\nu T = 10^{-3}$. In our case the optimum modulation index is found to be $h = 0.9$ for the same value of linewidth. It is noticed that there is close agreement between the two curves which proves the validity of the assumptions made in carrying out the theoretical analysis.

2.7 Summary

A simplified theoretical analysis is presented for an optical heterodyne CPFSK delay-demodulation system. A formulation is developed to evaluate the bit error performance of the system taking into account the effect of laser phase noise, receiver noise and non-uniform LD FM response. The analysis is extended to AMI linecoded CPFSK system in order to investigate the effectiveness of linecoding in overcoming the pattern dependent modulation effect arising due to non-uniform LD FM.

Based on the theoretical formulation, the bit error performance of an optical heterodyne CPFSK delay-demodulation receiver is evaluated. It is observed that the system performance is highly degraded with non-uniform LD FM response and exhibits a bit error floor. The performance can not be improved by increasing the modulation index. But significant improvement can be achieved by using AMI linecoding and the power penalty can be greatly reduced to 2.2 dB with optimum modulation index of 0.9 and normalized linewidth $\Delta\nu T = 10^{-3}$. It is also found that the obtained results are in good agreement with the experimental results [33].

CHAPTER 3

SIMULATION OF OPTICAL CPFSK HETERODYNE RECEIVER WITH DELAY-DEMODULATION

3.1 Introduction

The theoretical analysis of an optical heterodyne CPFSK delay-demodulation system is presented in chapter 2. The performance evaluation of the system through exact theoretical analysis become complicated when the transmitting laser has a non-uniform FM response characteristics as well as nonzero linewidth. The alternate way to the theoretical analysis is the detailed experimentation. The experimentation on the system can be performed through either hardware implementation or computer simulation. The hardware implementation of the system is much more complex, expensive and time consuming compared to computer simulation. An added advantage of computer simulation is the insight obtained into the system behavior while realizing the various physical process of the system through back-by-back implementation.

In this chapter, a computer simulation method is presented for the performance evaluation of optical heterodyne CPFSK delay-demodulation system, taking into account the effect of laser phase noise, receiver noise and the non-uniform FM response of the transmitting DFB laser. The simulation is carried out for random NRZ and AMI encoded data. Starting from the IF signal, statistical Monte-Carlo simulation of the system is carried out using the technique of 'composite importance sampling'.

3.2 Modified Monte-Carlo Simulation

Monte-Carlo simulation allows one to analyze the effects of several impairments in the system. The main problem with Monte-Carlo simulation is the large sample size required for estimating low error probabilities. Estimation of error probability of the order of P_e , with a normalized estimation error of $1/3$, requires a sample size of the order of $10/P_e$ [34]. Several techniques have been developed to reduce the sample size requirement. Some techniques are based on the asymptotic approximation of the tail probabilities of a distribution which can reduce the sample size requirement.

The modified Monte-Carlo simulation utilizes importance sampling technique which is based on a biased sampling scheme [28-30]. The estimation of samples that occur infrequently may require considerable or even prohibitive, computational effort. Importance sampling is a technique that permits simulation of low probability samples with major reduction of the computational effort required. The basic principle is to make the samples of interest to occur more frequently than normal. This is done by modifying or biasing the probability density function (pdf) of the noise process so that the samples of interest occur with increased probability while the samples that are not of interest occur with reduced probability. The bias associated with each sample of the noise sequence is determined from the amount of increase in probability. In this way, the same estimator variance can be obtained with fewer trials than is required for direct Monte-Carlo simulation. Alternatively, a smaller estimator variance can be obtained with the same number of trials required by direct Monte-Carlo simulation.

3.2.1 Biasing a Gaussian Pdf

A noise process with Gaussian pdf is shown in figure 3.1. The noise process has variance σ^2 and mean zero. So the pdf of this noise process is

$$f_X(x) = \frac{1}{\sqrt{2\pi}\sigma} \exp\left(-\frac{x^2}{2\sigma^2}\right) \quad (3.1)$$

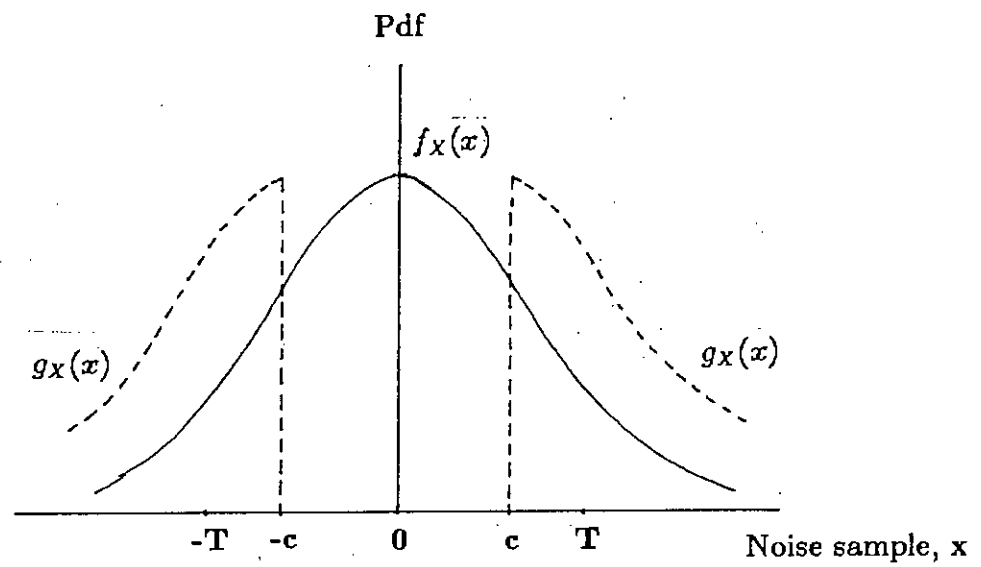


Figure 3.1: The original pdf $f_X(x)$ and the transformed pdf $g_X(x)$.

In order to estimate the error probability due to the noise samples at the tail of the Gaussian pdf, the pdf $f_X(x)$ is modified to $g_X(x)$ to increase the tail probability. The positive samples are incremented by c and the negative samples are decremented by c ($c \leq T$) [36],

$$\begin{aligned} X' &= X + c, & X \geq 0 \\ &= X - c, & X < 0 \end{aligned} \quad (3.2)$$

where the threshold T is selected to give a desired error probability. The error probability is given by

$$P_e = Q\left(\frac{T}{\sigma}\right) \quad (3.3)$$

where

$$Q(x) = \frac{1}{\sqrt{2\pi}} \int_x^{\infty} \exp\left(-\frac{\alpha^2}{2}\right) d\alpha \quad (3.4)$$

The pdf of the modified noise process will be

$$\begin{aligned} g_X(x) &= \frac{1}{\sqrt{2\pi}\sigma} \exp\left[-\frac{(x-c)^2}{2\sigma^2}\right], & x \geq c \\ &= \frac{1}{\sqrt{2\pi}\sigma} \exp\left[-\frac{(x+c)^2}{2\sigma^2}\right], & x \leq -c \end{aligned} \quad (3.5)$$

Now errors will occur more frequently with X' than with X . If a sample X_k is selected from $g_X(x)$, its probability is increased by $B(X_k) = g_X(X_k)/f_X(X_k)$ and the bias associated with the k th sample is given by [36],

$$\begin{aligned} B(X_k) &= \exp\left[\frac{c(2X_k - c)}{2\sigma^2}\right], & X_k \geq c \\ &= \exp\left[-\frac{c(2X_k + c)}{2\sigma^2}\right], & X_k \leq -c \end{aligned} \quad (3.6)$$

3.2.2 Weighting Factor

If an error occurs due to X' , it will be an enhanced error. To get the actual error, the error count will have to be weighted by $W(X_k) = \frac{1}{B(X_k)}$. For a system with memory

of length L , the output variable Y is a function of L independent variables, i.e.,

$$Y = f(X_1, X_2, X_3, \dots, X_L) \quad (3.7)$$

Now a sample Y_i is determined by L independent input samples, $Y_i = f(X_{1i}, X_{2i}, X_{3i}, \dots, X_{Li})$. So the probability of Y_i is increased (or decreased) by the product of the biases of L input samples. So the weighting factor for Y_i will be

$$W_i = \left[\prod_{m=1}^L B_{mi} \right]^{-1} \quad (3.8)$$

3.3 Steps of Simulation

The block diagram of a heterodyne delay-demodulation receiver shown in figure 2.3 is used in the simulation. The optical frequencies are of the order of 10^{14} Hz. The computer will not support to deal with such very high frequency signal samples. Therefore, simulation is started from the IF signal. The effect of laser phase noise, receiver noise and non-uniform FM response of transmitting DFB laser are taken into consideration. The bit error rate (BER) is estimated for different conditions. The steps of the simulation procedure are presented here.

3.3.1 Generation of IF Signal Samples

The signal at the input of IF filter, i.e. the IF signal, is given by

$$\begin{aligned} r(t) &= S \cos[2\pi f_{IF}t + \phi_s(t) + \phi_n(t)] + n(t) \\ &= s(t) + n(t) \end{aligned} \quad (3.9)$$

where

$$S = \text{amplitude} = 2R\sqrt{P_S P_{LO}},$$

R = responsivity of the photodetector,

P_S, P_{LO} = power of input signal and of local oscillator signal respectively,

$\phi_s(t)$ = angle modulation,

$\phi_n(t)$ = composite phase noise of transmitting and local oscillator laser, and

$n(t)$ = complex additive Gaussian noise of variance σ^2 .

The signal samples at an interval of T_s seconds is

$$\begin{aligned} \{r(iT_s)\} &= S \cos[2\pi f_{IF}iT_s + \phi_s(iT_s) + \phi_n(iT_s)] + n(iT_s) \\ &= S \cos\left[2\pi f_o \frac{i}{N_{SB}} + \phi_s(iT_s) + \phi_n(iT_s)\right] + n(iT_s) \end{aligned} \quad (3.10)$$

where, $T_s = \frac{T}{N_{SB}}$, T is the bit period, N_{SB} is the number of samples per bit and $f_o = f_{IF}T$ is the normalized IF frequency.

3.3.2 Generation of Bit Sequence

A sequence of random information bit $\{a_n\}$ is generated by using a $(2^N - 1)$ pseudorandom bit sequence (PRBS) generator where N is the length of the sequence. An N -bit shift register with suitable feedback is used to generate pseudorandom bit sequence. The inputs to the feedback network are the outputs at selected stages of the register. The stages are selected to yield the maximum length of the bit sequence. Thus a generator with 23-bit shift register can generate a sequence of $(2^{23} - 1)$ bits [37].

3.3.3 Generation of Angle Modulation Samples

The angle modulation is given by

$$\phi_s(t) = 2\pi \int_{-\infty}^t [I(t) * m(t)] dt \quad (3.11)$$

where $I(t)$ is the NRZ information bit sequence and $m(t)$ is the FM impulse response of the transmitting laser. The information bit sequence $I(t)$ is given by

$$I(t) = \sum_{n=-\infty}^{\infty} a_n p(t - nT) \quad (3.12)$$

where a_n is the n th information bit and $p(t)$ is the elementary pulse shape. Then the i th sample of the n th bit (k th signal sample) is given by

$$I(kT_s) = a_n p(iT_s) \quad (3.13)$$

where

$$k = (n-1)N_{SB} + i, \quad i = 1, 2, \dots, N_{SB},$$

$p(iT_s)$ = sampled version of the pulse shape $p(t)$.

The non-uniform FM response, $M(f)$ of the transmitting laser is sampled at an interval of F_s Hz to obtain the sampled version of $M(f)$, i.e. the sequence $\{M(iF_s)\}$. The value of F_s is determined by the nature of the non-uniform FM response $M(f)$ and the accuracy of estimation. In this simulation, the FM response of a DFB laser shown in figure 2.1 is considered and the value of F_s is taken to be 10 kHz.

Now the samples $\{I(iF_s)\}$ and $\{M(iF_s)\}$ are multiplied and then the inverse Fourier transformation of these multiplied samples is taken to obtain the samples $\{c(iT_s)\} = \{I(iT_s)\} * \{m(iT_s)\}$. Then the k th sample of angle modulation signal is obtained as

$$\begin{aligned} \phi_s(kT_s) &= 2\pi \sum_0^{N_{SB}} c(iT_s)T_s \\ &= \frac{2\pi T}{N_{SB}} \sum_0^{N_{SB}} c(iT_s) \end{aligned} \quad (3.14)$$

where

$$k = (n-1)N_{SB} + i, \quad i = 1, 2, 3, \dots, N_{SB}$$

3.3.4 Generation of Phase Noise Samples

It is convenient to generate the phase noise samples from the equivalent frequency noise process. The samples of the phase noise process $\phi_n(t)$ are therefore represented by

$$\phi_n(kT_s) = \sum_{i=0}^k \phi'_n(iT_s) 2\pi T_s \quad (3.15)$$

where $\phi'_n(t) = \frac{d\phi_n(t)}{dt}$, $\phi'_n(iT_s)$ is the i th sample of the frequency noise $\phi'_n(t)$ which is generated by a random number generator following a Gaussian distribution having zero mean and variance $\Delta\nu B_e/2\pi$ where $\Delta\nu$ is the total linewidth of the lasers and B_e is the effective IF filter bandwidth [14].

3.3.5 Generation of Noise Samples

The noise samples $\{n_k\}$ are generated by using a random number generator. The noise samples $\{n_k\}$ and their associated biases $\{b_k\}$ are generated by importance sampling [36] using a biased Gaussian pdf of zero mean and variance $\sigma_i^2 = (f_s/B_e)\sigma_o^2$, where f_s is the sampling frequency and σ_o^2 is the noise variance at the IF filter output. The IF signal-to-noise ratio is defined as $\xi = FA^2/\sigma_o^2$, where F is the IF bandwidth expansion factor ($= B_{IFT}$).

The procedure for pseudorandom number generation used in the simulation is known as the congruential method, proposed by Lehmer in 1951 [39]. There are two forms of congruential method. Here the multiplicative method is used which has the following recurrence relationship,

$$X_{i+1} = aX_i \pmod{m} \quad (3.16)$$

The method takes the last random number X_i , multiplies it by a constant a , and takes the result, modulo m (that is, divides by m and treats the remainder as X_{i+1}). Thus the random numbers all range between zero and $(m - 1)$. m is chosen as the largest possible integer in the computer so that division to take the modulo is done implicitly by the multiplication process and some computer time is saved.

The random numbers thus generated can be converted to random variate with a Gaussian distribution by using the central limit theorem. If the random numbers X_i have mean μ_x and variance σ_x^2 then the random variate with Gaussian variate will be

87792

[38]

$$Y = \sigma_x \frac{\sqrt{12}}{K} \left[\sum_{i=1}^K X_i - \frac{K}{2} \right] + \mu_x \quad (3.17)$$

The minimum value of K , to satisfy the central limit theorem, is 10. However, $K = 12$ is a good choice.

3.3.6 IF Filtering

The signal samples and noise samples are combined together. This contaminated signal is to be passed through an IF filter. In this simulation, the sequence of samples $\{Y_k\}$ at the IF filter output are obtained by convolving the input sequence $\{X_k\} = \{S_k\} + \{n_k\}$, with the IF filter impulse response $\{h_k\}$ using a Fast Fourier transform (FFT) routine.

The IF filter is considered to be a bandpass integrator with integration time $T' = \frac{T}{F}$ where T is the bit period and F is the IF bandwidth expansion factor. Other shapes of the IF filter may be considered. However, different filters behave more or less similar if their equivalent bandwidths remain the same. Then the impulse response of the IF filter is

$$\begin{aligned} h(t) &= \frac{1}{T'} \cos(2\pi f_{IF} t), \quad 0 \leq t \leq T' \\ &= 0, \quad \text{elsewhere.} \end{aligned} \quad (3.18)$$

The bias associated with the output samples $\{Y_k\}$ are obtained as

$$B_o(Y_k) = \prod_{j=1}^L B(X_{k+1-j}) \quad (3.19)$$

where L is the memory length of the IF filter impulse response.

3.3.7 Delay-demodulation

The digital information is detected from the IF output signal through delay-demodulation method. The signal is time-delayed by $\tau = \frac{T}{2h}$ where h is the modulation

index ($= 2\Delta fT$). The delayed samples are multiplied with the original samples.

The delay-demodulated signal is passed through a low-pass filter. Here the sequence of samples at the low-pass filter output are obtained by convolving the input signal samples with the impulse response of the low-pass filter by using an FFT routine. The impulse response of the low-pass filter is considered to be rectangular with bandwidth equal to the bit rate.

3.3.8 Computation of BER

For NRZ data the output samples at the middle of each bit period are compared to a threshold of zero value to determine the output bit sequence. This bit sequence is then compared to the transmitted bit sequence and the errors are counted.

The bit error rate (BER) is computed for an N-bit sequence as follows,

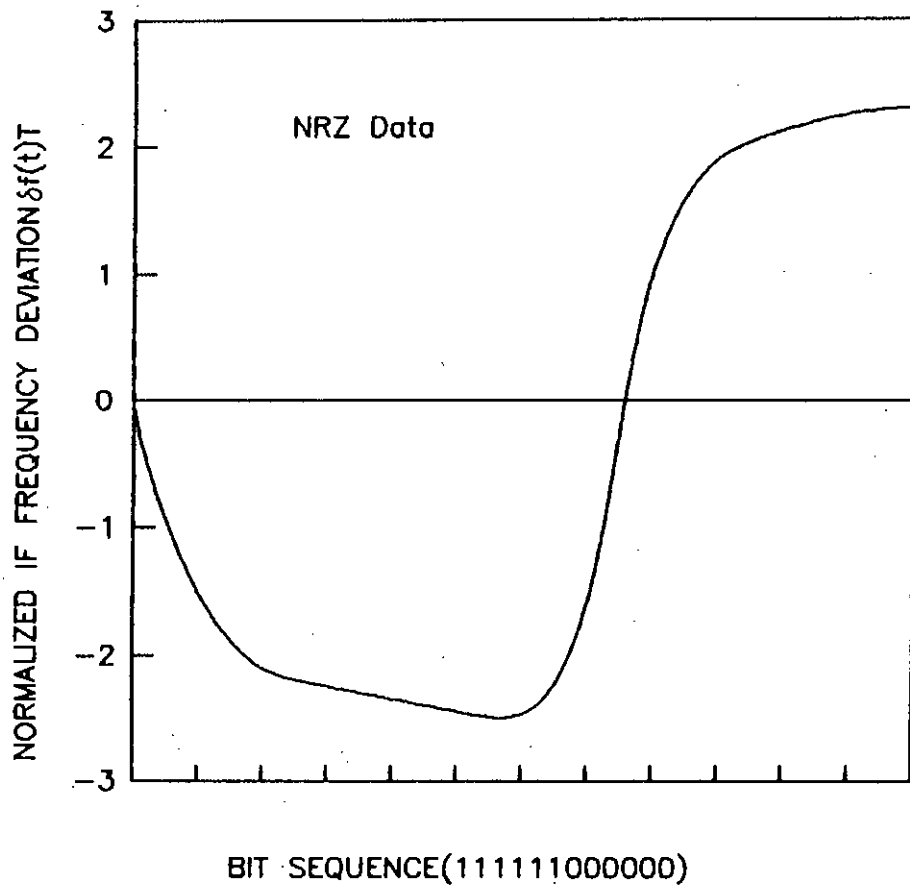
$$P_b = \frac{1}{N} \sum_{i=1}^N u_i \quad (3.20)$$

where u_i is zero if the i th bit is received correctly, or is equal to W_i if it is received with error, where W_i is the reciprocal of the bias corresponding to the output sample at the end of the i th bit period.

For AMI encoded data the decoding is carried out by considering two consecutive output bits.

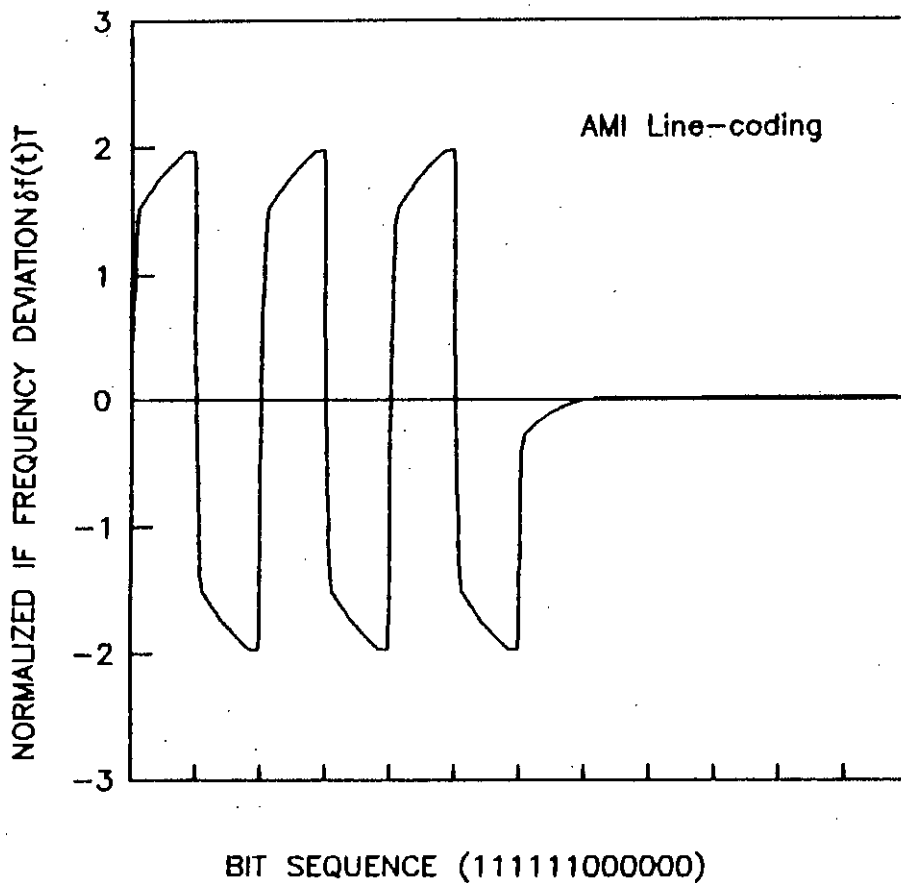
3.4 Results and Discussions

In this section we present the results obtained by modified Monte-Carlo simulation of optical heterodyne CPFSK delay-demodulation system taking into consideration the effects of laser phase noise, receiver noise and non-uniform LD FM response. The FM response of a DFB laser used for theoretical computation is also used for simulation. Simulation is carried out for both NRZ and AMI encoded data for $(2^{23} - 1)$ PRBS at a bit rate of 2.5 Gb/s with IF bandwidth of 5.0 GHz.



(a)

Figure 3.2: IF frequency deviation with non-uniform LD FM response
 (a) for NRZ data



(b)

Figure 3.2: (contd.)
 (b) for AMI encoded data.

Figure 3.2 shows the waveform of IF deviation at the output of the IF filter for both NRZ and AMI data pattern. The non-uniform FM response causes the IF deviation to continue upto a number of bits. The figure is shown for a 111...000... data pattern and it shows that for continuous 1's or for continuous 0's there is continuous drift in the IF deviation and thus the IF waveform becomes distorted. The distortion is severe in case of random NRZ data. In contrast, there is a little distortion in the IF waveform and there is no tendency for frequency drift for long strings of 1's or 0's, when AMI linecoding is employed.

With the laser FM response shown in figure 2.1 and other system parameters mentioned in section 2.6, both theoretical and simulation performance results for CPFSK system with and without linecoding are shown in figure 3.3. These sets of results correspond to the case of zero phase noise ($\Delta\nu T = 0.0$) and IF filter bandwidth equal to twice the bit rate. We report the results for two values of modulation index h , viz. 1.0 and 1.15 for NRZ data and $h = 1.0$ for AMI encoded data. It is noticed from the simulation results that CPFSK system with NRZ data experiences an error rate floor at about $BER=3 \times 10^{-5}$ and 5×10^{-4} for $h = 1.15$ and $h = 1.0$ respectively. No error rate floor occurs when the CPFSK system uses linecoded data or 1010 data pattern. For 1010 data pattern with $\Delta\nu T = 10^{-3}$, there is a penalty of only 1 dB relative to 'ideal FM' case. We also notice a good agreement between the theoretical and simulation results, as the corresponding curves are within 1 dB from each other.

When phase noise is included along with non-ideal FM response, the theoretical performance results and the corresponding results for the linecoded CPFSK systems are shown in figure 3.4 as a function of IF SNR for three values of normalized linewidth $\Delta\nu T = 10^{-4}$, 10^{-2} and 5×10^{-2} with modulation index h set to 0.9. It is noticed from theoretical results that the penalties suffered at $BER=10^{-9}$ by AMI-FSK are 2.05 dB dB and 5.1 dB relative to the 'ideal FM' performance for $\Delta\nu T = 10^{-4}$ and 10^{-2} respectively. The corresponding penalty estimates from the simulation are about 2.8 dB

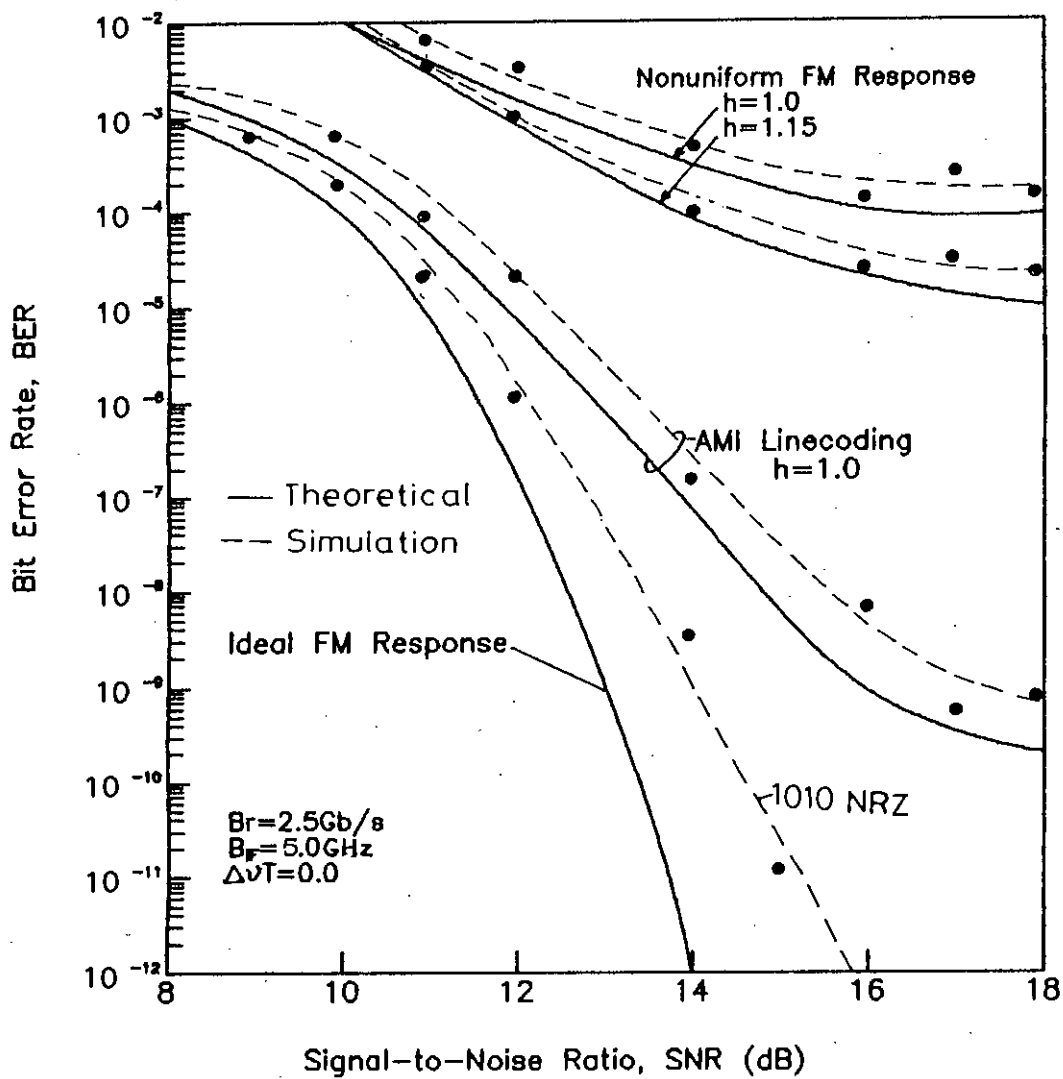


Figure 3.3: Comparison of theoretical and simulation results for bit error rate of optical CPFSK system with $\Delta\nu T = 0.0$

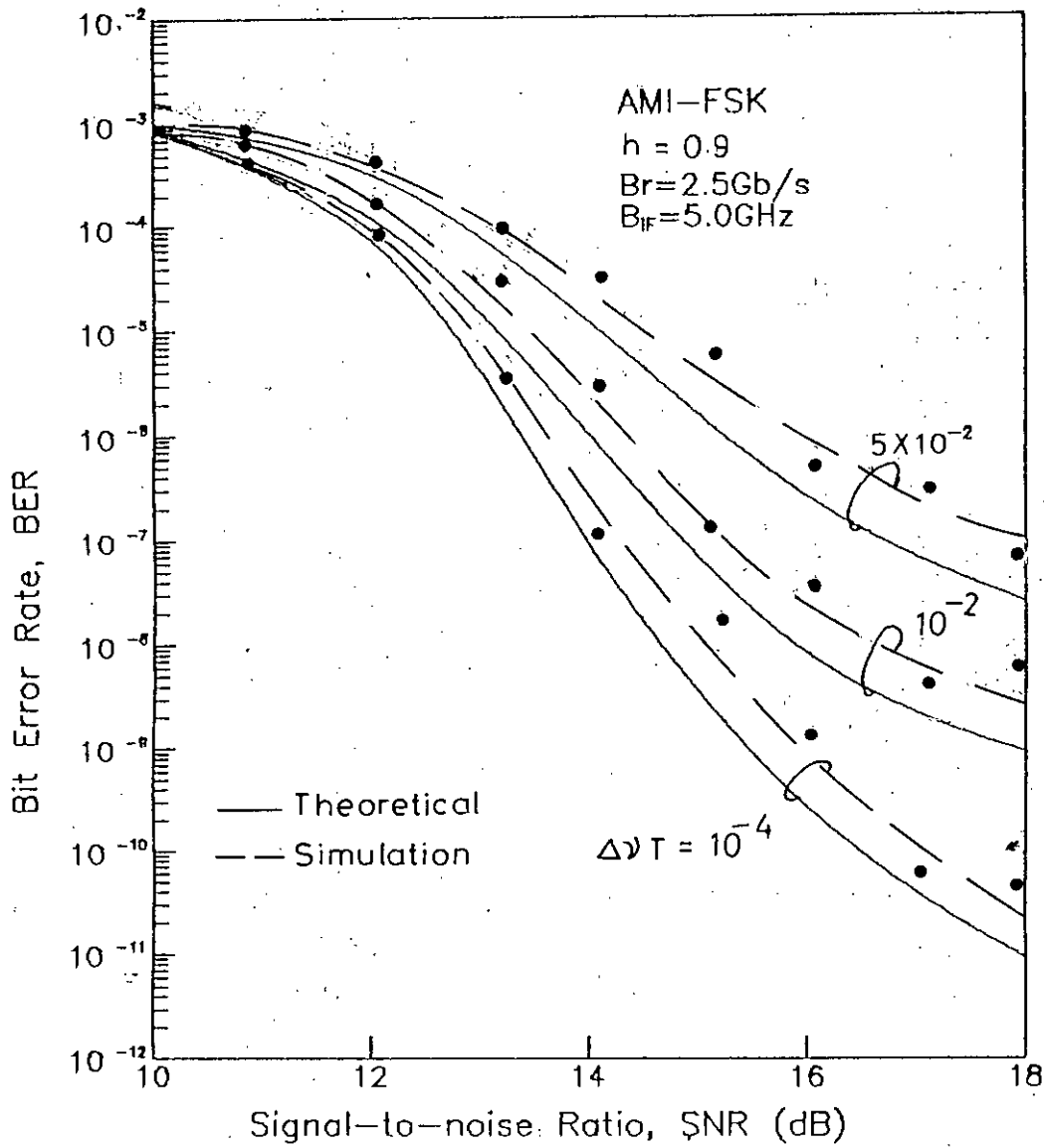


Figure 3.4: Comparison of theoretical and simulation results for bit error rate of optical CPFSK system with AMI coded data for several values of linewidth with modulation index $h=0.9$

and 5.8 dB respectively. Thus there is a close conformity among the theoretical results and results obtained by simulation. These values are well confirmed by experimental results reported in Reference 4.

3.5 Summary

A statistical Monte-Carlo simulation technique for optical heterodyne CPFSK receiver with delay-demodulation is presented in this chapter. The 'composite importance sampling' technique is employed to reduce the sample size and computation time.

The bit error probability is estimated for the CPFSK delay-demodulation receiver for 'ideal FM' case and for 'non-ideal FM' case. The simulation also includes the effects of laser phase noise and receiver noise.

The theoretical results are compared with simulation results and a good agreement between them is observed. The simulation results are also verified by the experimental results reported earlier.

CHAPTER 4

CONCLUSIONS AND SUGGESTIONS

4.1 Conclusions

The performance of an optical heterodyne CPFSK system with delay-demodulation has been investigated in this work. The major problems of optical CPFSK system considered are

i) receiver noise containing shot and thermal noises which is modeled as additive white Gaussian noise,

ii) laser phase noise arising due to the non-zero linewidth of the laser output,

iii) non-uniform frequency modulation (FM) characteristic of transmitting distributed feedback (DFB) semiconductor laser diode (LD) which causes the pattern dependent bit error rate performance.

In chapter 2, a theoretical analysis of an optical heterodyne CPFSK receiver with delay-demodulation is presented. The theoretical formulation is developed to evaluate the impact of non-uniform FM response of a practical DFB laser on the bit error performance of the system. The analysis also includes the effects of additive receiver noise and laser phase noise of transmitting and local oscillator lasers due to non-zero linewidth.

The theoretical analysis is extended to optical heterodyne CPFSK system with Alternate-Mark-Inversion (AMI) linecoded data. The AMI linecoding is utilized to investigate the effectiveness of linecoding in counteracting the effect of non-uniform LD FM response and hence to reduce the pattern dependent modulation effect.

The FM response $M(f)$ of a practical DFB laser, as shown in figure 2.1, is used for numerical computations of the system performance. The effective pulse shapes for NRZ data and for AMI encoded data are determined and are found to be distorted due to the non-uniform LD FM response. The non-uniform LD FM response produces a random phase fluctuation at the output of the discriminator. The pdf of the random phase error at the demodulator output is determined without linecoding for several values of modulation index. Using the pdf, the bit error probability for the CPFSK receiver is evaluated for both NRZ and AMI encoded data. The system is found to suffer a bit error floor due to non-flat FM response and laser phase noise. The floor is at much higher values, of the order of 10^{-4} , for NRZ data and can not be significantly lowered by increasing the modulation index. Thus the bit error rate of 10^{-9} can never be achieved. The minimum attainable bit error rate floor occurs at about 10^{-5} corresponding to an optimum value of modulation index equal to 1.15. On the otherhand, the system performance is significantly improved when AMI linecoding is utilized. The error rate floor can be significantly lowered to 10^{-9} or even lower values by increasing the value of modulation index and the system suffers a penalty of only 2.0 dB relative to 'ideal FM case' at optimum value of modulation index $h = h_{opt} = 0.9$ in the absence of laser phase noise. Further increase in modulation index causes the bit error floor and the penalty to increase. In the presence of laser phase noise the system suffers penalty due to the combined effect of laser phase noise and non-uniform FM response. The additional penalty, compared to the system without phase noise, increases with increasing linewidth. At a given linewidth there is an optimum modulation index for which penalty reaches its minimum value.

The theoretical results are compared with the theoretical and experimental results reported earlier in a published work [33]. It is noticed that there is a close agreement between our results and the published results.

Finally, a detailed Monte-Carlo simulation of the system is carried out for the same

receiver and system parameters as in theoretical computations. The technique of 'importance sampling' is utilized for considerable reduction in sample size and computation time. It is found that the results obtained by computer simulation are in good agreement with those obtained theoretically and thus prove the validity of the assumptions taken in the theoretical formulation.

4.2 Suggestions

In the present work, the performance of a CPFSK delay-demodulation system with NRZ and AMI encoded data is studied. There are other linecoding techniques, for example delay modulation (DM) or Miller code, Manchester code (MC), used in optical communication. The theoretical analysis and simulation study can be extended to investigate the effects of such linecoding techniques in overcoming the effect of non-uniform LD FM response.

As the optical signal received at the receiver front-end is significantly weak, optical preamplifier can be utilized before photodetection. But additional noises will then arise due to beating of signal with spontaneous emission in the amplifier. The analysis will have to account for these noises.

The work has been carried out on single-channel optical CPFSK system. Further work can be pursued on multi-channel optical CPFSK system. In multi-channel system, Mach-Zehnder interferometer can be employed as an optical discriminator. The effect of non-uniform LD FM response on the performance of optical multi-channel FSK system and the use of linecoding in reducing this effect can be studied. The performance degradation of multi-channel transmission due to nonlinear effects of optical fibres, namely, chromatic dispersion, can be investigated. Further study can be carried out to evaluate the effect of four-wave mixing on optical frequency division multiplexing (OFDM) system.

REFERENCES

- [1] Tingye Li, "Optical Fibre Communication- The State of the Art", IEEE Trans. Commun. vol. COM-26, no. 7, July 1978, pp. 946-954.
- [2] Gerd Keiser, "Optical Fibre Communication", McGraw-Hill Book Company, New York, 1983.
- [3] S. P. Majumder, "Theoretical and Simulation Studies on Some Relevant Modulation Schemes in Direct Detection and Coherent Optical Communication Systems", Ph.D. Dissertation, Indian Institute of Technology, Kharagpur(India), November 1991.
- [4] K. Iwashita and T. Matsumoto, "Modulation and Detection Characteristics of Optical Continuous Phase FSK Transmission System", J. Lightwave Technol., vol. LT-5, April 1987, pp.461-468.
- [5] T. Okoshi, K. Emura, K. Kikuchi and R. T. Kersten, "Computation of Bit Error Rate of Various Heterodyne and Coherent Type Optical Communication Schemes", J. Opt. Commun., vol. 2, no. , 1981, pp.89-9. pp. 137-180.
- [6] T. G. Hodgkinson, "Receiver Analysis for Synchronous Coherent Optical Fibre Transmission Systems", J. Lightwave Technol., vol. LT-5, no. 4, 1987, pp. 573-586.
- [7] G. J. Foschini, L. J. Greenstein and G. Vannucci, "Noncoherent Detection of Coherent Lightwave Signals Corrupted by Phase Noise", IEE Trans. Commun., vol. COM-36, March 1988, pp. 306-314.
- [8] L. G. Kazovsky, "Impact of Laser Phase Noise on Optical Heterodyne Communication Systems", J. Opt. Commun., vol.7,1986, pp. 66-77.

- [9] I. Garrett and G. Jacobsen, "The Effect of Laser Linewidth on Coherent Optical Receivers with Non-synchronous Demodulation", *J. Lightwave Technol.*, vol. LT-5, no. 4, 1987, pp. 551-560.
- [10] K. Emura, et. al., "System Design and Long Span Transmission Experiments on Optical FSK Heterodyne Single Filter Detection System", *J. Lightwave Technol.*, vol. LT-5, no. 4, April 1987, pp. 469-477.
- [11] S. Saito, Y. Yamamoto and T. Kimura, "S/N and Error Rate Evaluation for an Optical FSK Heterodyne Detection System using Semiconductor Lasers", *IEEE J. Quantum Electron.*, vol. QE-19, 1983, pp. 180-192.
- [12] K. Kikuchi, T. Okoshi, T. Nagamatsu and N. Henmi, "Degradation of Bit Error Rate in Coherent Optical Communications due to Spectral Spread of the Transmitter and Local Oscillator", *J. Lightwave Technol.*, vol. LT-2, no. 6, 1984, pp. 1024-1033.
- [13] I. Garrett and G. Jacobsen, "Theoretical Analysis of Heterodyne Optical Receivers for Transmission Systems using (Semiconductor) Laser with Non-negligible Linewidth", *J. Lightwave Technol.*, vol. LT-4, no. 3, March 1986, pp. 323-334.
- [14] I. Garrett and G. Jacobsen, "Statistics of Laser Frequency Fluctuations in Coherent Optical Receivers", *Electron. Lett.*, vol. 22, 1986, pp. 168-170.
- [15] I. Garrett and G. Jacobsen, "Theory for Optical Heterodyne Narrow-Deviation FSK Receivers with Delay Demodulation", *J. Lightwave Technol.*, vol. LT-6, 1988, pp. 1415-1423.
- [16] R. J. S. Pedersen, I. Garrett and G. Jacobsen,, "Measurement of Statistics of DFB Laser Fluctuations", *Electron. Lett.*, vol. 24, 1988, pp. 585-586.

- [17] N. A. Olsson, "Lightwave Systems with Optical Amplifiers", *J. Lightwave Technol.*, vol. 7, no. 7, July 1989, pp. 1071-1082.
- [18] Y. Yoshikuni and G. Motosugi, "Multielectrode Distributed Feedback Laser for Pure Frequency Modulation and Chirping Suppressed Amplitude Modulation", *J. Lightwave Technol.*, vol. LT-5, no. 4, April 1987, pp. 516-522.
- [19] S. B. Alexander and D. Welford, "Equalization of Semiconductor Laser Diode Frequency Modulation with a Passive Network", *Electron. Lett.*, vol. 21, 1985, pp. 361-362.
- [20] Y. Yamazaki, K. Emura, M. Shikada, M. Yamaguchi and I. Mito, "Realization of Flat FM Response by Directly Modulating a Phase Tunable Laser Diode", *Electron. Lett.*, vol. 21, 1985, pp. 283-285.
- [21] B. Enning and R. S. Vodhanel, "Adaptive Quantized Feedback Equalization for FSK Heterodyne Transmission at 150 Mbit/s and 1 Gbit/s", in *Tech. Dig. Opt. Fibre Commun. Conf.*, (New Orleans, LA), 1988, postdeadline pap. PD23.
- [22] K. Emura et. al., "Novel Optical FSK Heterodyne Single Filter Detection System using a Directly Modulated DFB Laser Diode", *Electron. Lett.*, vol. 24, 1985, pp. 1022-1023.
- [23] R. Noe., "AMI Signal Format for Pattern Independent FSK Heterodyne Transmission and Two Channel Crosstalk Measurements", *J. Opt. Commun.*, vol. 10, 1989, pp. 82-84.
- [24] P. W. Hooijmans, M. T. Tomesen and A. V. De Grijp, "Penalty Free Biphasic Linecoding for Pattern Independent FSK Coherent Transmission System", *J. Lightwave Technol.*, vol. 8, no. 3, March 1990, pp. 323-328.

- [25] B. Glance, "Polarization Independent Coherent Optical Receivers", *J. Lightwave Technol.*, vol. LT-5, no.2, 1987, pp. 274-276.
- [26] J. M. Osterwalder and B. J. Rickett, "Frequency Modulation of GaAlAs Injection Lasers at Microwave Frequency Rates", *IEEE J. Quantum Electron.*, vol. QE-16, March 1980, pp. 250-252.
- [27] K. Emura, et.al., "Optimum System Design for CPFSK Heterodyne Delay Demodulation System with DFB LD's", *J. Lightwave Technol.*, vol. 8, no. 2, February 1990, pp. 251-258.
- [28] G. L. Abbas, V. W. S. Chan and T. K. Yee, "A Dual-Detector Optical Heterodyne Receiver for Local Oscillator Noise Suppression", *J. Lightwave Technol.*, vol. LT-3, 1985, pp. 1110-1122.
- [29] G. Jacobsen and I. Garrett, "Theory for Heterodyne Optical ASK Receivers using Square-law Detection and Postdetection Filtering", *IEEE Proc. J.*, vol. 134, 1987, pp. 303-312 (erratum= vol. 135, p.100,1988).
- [30] I. Garrett, G. Jacobsen and R. J. S. Pedersen, "Filtered Laser Beat Frequency Fluctuations", *IEEE Proc. J.*, vol. 135, 1988, pp. 408-412.
- [31] A. B. Carlson, "Communication Systems", McGraw-Hill Book Company, New York, 1968.
- [32] E. Bedrosian and S. O. Rice, "Distortion and Crosstalk of Linearly Filtered, Angle-modulated Signal", *Proceedings of the IEEE*, vol. 56, no. 1, January 1968, pp. 2-14.
- [33] G. Jacobsen, K. Emura, T. Ono and S. Yamazaki, "Requirements for LD FM Characteristics in an Optical CPFSK System", *J. Lightwave Technol.*, vol. 9, no. 9, September 1991, pp. 1113-1123.

- [34] V. K. Prabhu, "Some Considerations of Error Bounds in Digital Systems", *Bell Syst. Tech. J.*, vol. 50, no. 10, 1971, pp. 3127-3150 .
- [35] G. Nicholson, "Probability of Error for Optical Heterodyne DPSK System with Quantum Phase Noise", *Electron. Lett.*, vol. 20, no.24, November 1984, pp. 1005-1007. (1991) pp. 37-58.
- [36] S. Benedetto, E. Biglieri and V. Castellani, "Digital Transmission Theory", Prentice-Hall Inc., New Jersey, 1987.
- [37] K. S. Shanmugan and P. Balaban, "A Modified Monte-Carlo Technique for Evaluation of Error Rate in Digital Communication Systems", *IEEE Trans. Commun.*, vol. COM-18, 1980, pp. 1917-1924.
- [38] D. Lu and K. Yao, "Improved Importance Sampling Technique for Efficient Simulation of Digital Communication Systems", *IEEE J. Select. Areas Commun.*, vol. 6, January 1988.
- [39] N. C. Beaulieu, "A Composite Importance Sampling Technique for Digital Communication System Simulation", *IEEE Trans. Commun.*, vol. 38, no. 4, April 1990, pp. 393-396.
- [40] B. S. Sonde, "Introduction to System Design using Interfaced Circuits", Wiley Eastern Limited, 1980.
- [41] W. G. Bulgren, "Discrete System Simulation", Prentice-Hall Inc., New Jersey, 1982.
- [42] J. R. Emshoff and R. L. Sisson, "Design and Use of Computer Simulation Models", Macmillan Publishing Co. Inc., New York, 1970.
- [43] G. Jacobsen and I. Garrett, "Performance of CP-FSK System with Tight I.F. Filtering", *IEEE Photonics Technol. Lett.*, vol. 2, no. 10, October 1990, pp. 747-749.

- [44] L. L. Jeromin and V. W. S. Chan, "M-ary FSK Performance for Coherent Optical Communication System using Semiconductor Lasers", *IEEE Trans. Commun.*, vol. COM-34, no. 4, April 1986, pp. 375-381.
- [45] G. J. Foschini and G. Vannucci, "Characterizing Filtered Lightwaves Corrupted by Phase Noise", *IEEE Trans. Information Theory*, vol. 34, no. 6, November 1988, pp. 1437-1448.
- [46] K. Emura et. al., "An Optical FSK Heterodyne Dual Filter Detection System for Taking Advantage of DFB LD Applications", *J. Lightwave Technol.*, vol. 8, no. 2, February 1990, pp. 243-250.
- [47] N. M. Blachman, "The Effect of Phase Error on DPSK Error Probability", *IEEE Trans. Commun.*, vol. COM-29, no. 3, 1981, pp. 364-365.
- [48] L. Jeromin, B. Reiffen and V. W. S. Chan, "Minimum Shift Keying for Frequency Modulation of Semiconductor Lasers for a 100Mbit/s Coherent Optical Communication System", in *Proc. Conf. Optical Fibre Communication (Atlanta, GA)*, February 1986, pp. 50-51.

APPENDIX

A.1 Flow Chart

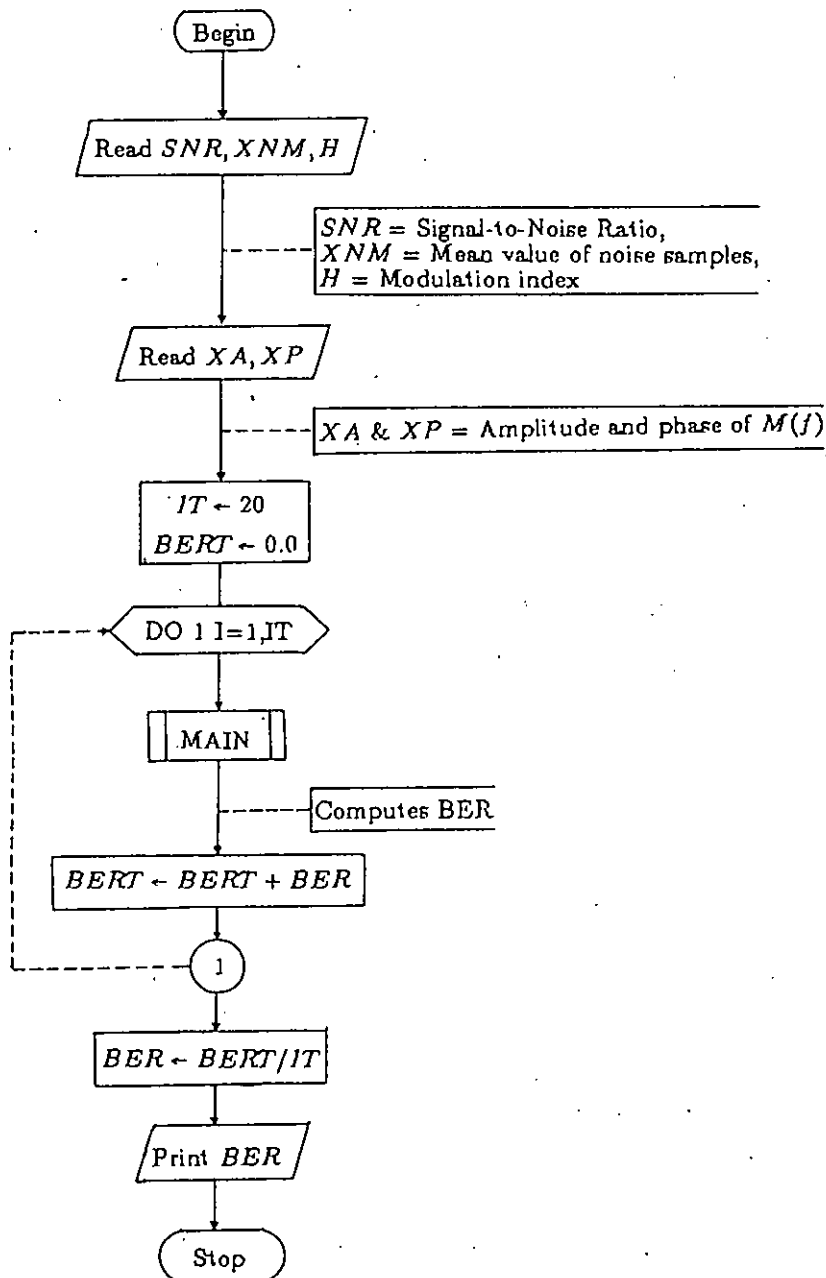


Figure A.1: Flow chart for computer simulation of optical heterodyne CPFSK system with delay-demodulation.

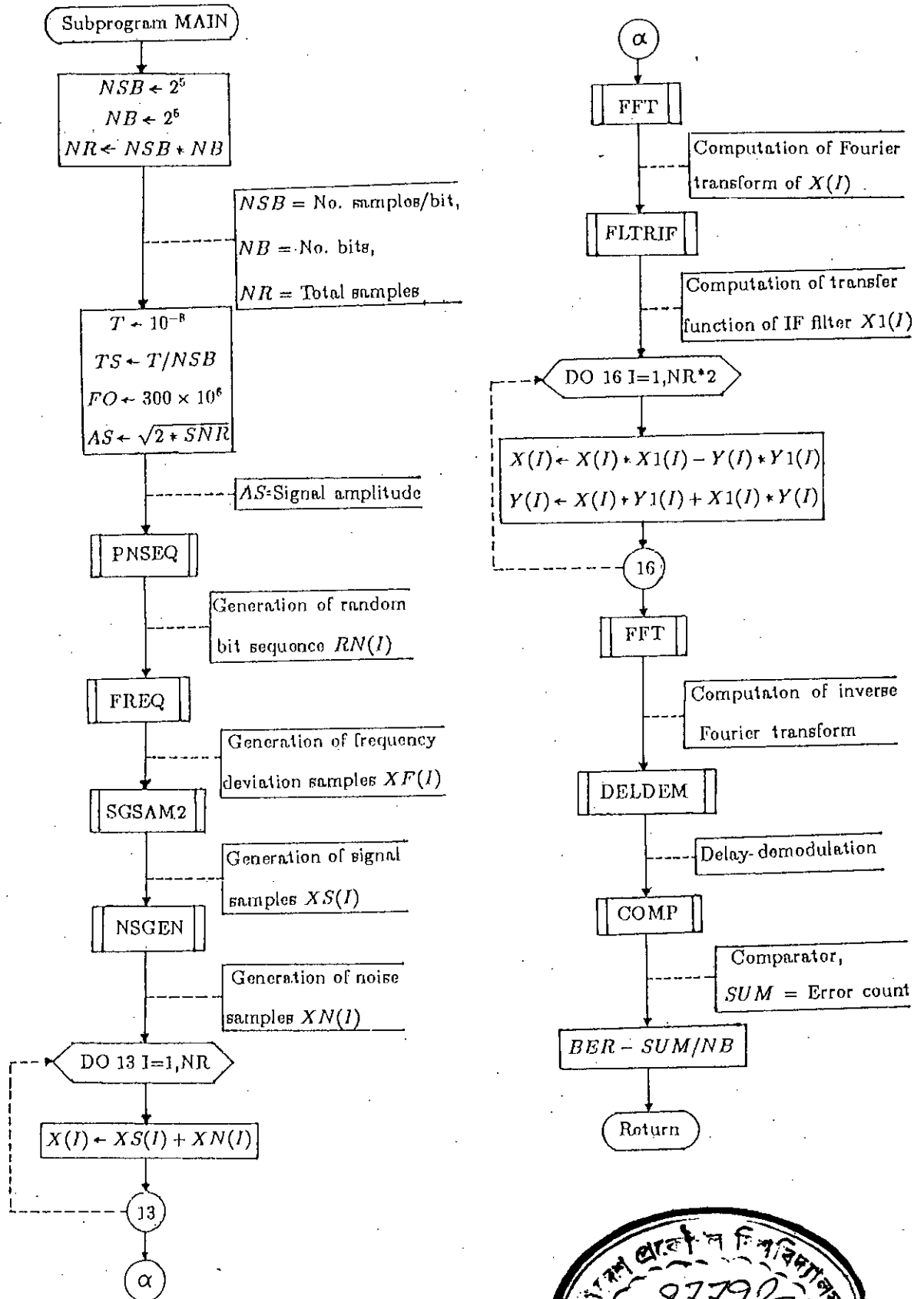


Figure A.1: (contd.).

